

# State-of-the-Art Design and Rapid-Mixing Production Techniques of Lipid Nanoparticles for Nucleic Acid Delivery

Martijn J. W. Evers, Jayesh A. Kulkarni, Roy van der Meel, Pieter R. Cullis, Pieter Vader, and Raymond M. Schiffelers\*

Lipid nanoparticles (LNPs) are currently the most clinically advanced non-viral carriers for the delivery of small interfering RNA (siRNA). Free siRNA molecules suffer from unfavorable physicochemical characteristics and rapid clearance mechanisms, hampering the ability to reach the cytoplasm of target cells when administered intravenously. As a result, the therapeutic use of siRNA is crucially dependent on delivery strategies. LNPs can encapsulate siRNA to protect it from degradative endonucleases in the circulation, prevent kidney clearance, and provide a vehicle to deliver siRNA in the cell and induce its subsequent release into the cytoplasm. Here, the structure and composition of LNP–siRNA are described including how these affect their pharmacokinetic parameters and gene-silencing activity. In addition, the evolution of LNP–siRNA production methods is discussed, as the development of rapid-mixing platforms for the reproducible and scalable manufacturing has facilitated entry of LNP–siRNA into the clinic over the last decade. Finally, the potential of LNPs in delivering other nucleic acids, such as messenger RNA and CRISPR/Cas9 components, is highlighted alongside how a design-of-experiment approach may be used to improve the efficacy of LNP formulations.

## 1. Introduction

The efficient delivery of nucleic acids to target cells *in vivo* is challenging due to their rapid degradation in biological media and rapid clearance from the circulation. In order to exert their function, nucleic acids are required to reach their target tissue within the body without alterations to their relatively complex structure (and sequence), and subsequently, the cytosol and/

or nucleus of target cells. As free nucleic acids are rapidly degraded by endonucleases and cleared by the kidney, reaching the target site as a functional molecule is unlikely.<sup>[1]</sup> Therefore, delivery systems are required to truly capitalize on the therapeutic potential of nucleic acid payloads. Lipid nanoparticles (LNPs) represent the most clinically advanced nonviral vectors for delivery of therapeutic small interfering RNA (siRNA).<sup>[2]</sup> Recently, an LNP–siRNA formulation for the treatment of transthyretin-induced amyloidosis (Patisiran) met all primary and secondary endpoints in a Phase-III clinical trial.<sup>[3]</sup> The sponsor (Alnylam Pharmaceuticals) applied for market access in late 2017 which will, if approved, mark the first LNP–siRNA therapeutic.<sup>[4]</sup> Additionally, LNPs encapsulating siRNA treating other liver diseases have entered the clinic and are in Phase-I/II trials (Table 1).<sup>[2]</sup> Alongside LNP–siRNA development, formulations for the delivery of messenger RNA (mRNA) have also reached

clinical stages. The ongoing trials with various nanoparticle formulations are outlined in Table 1.

Functionally, siRNAs enable specific silencing of virtually any gene in the human genome via a mechanism referred to as RNA interference.<sup>[5–7]</sup> After reaching the cytoplasm, siRNA interacts with the RNA-induced silencing complex (RISC). The siRNA molecule is loaded into the argonaute 2 protein and unwound, after which the sense strand is discarded leaving the antisense strand loaded in the RISC.<sup>[8]</sup> mRNA with a complementary sequence to the antisense strand is degraded by the RISC complex resulting in decreased expression of the protein encoded by the target mRNA.<sup>[9]</sup> The broad therapeutic applicability of siRNA is evident by ×20 ongoing clinical trials for the treatment of different types of cancer, liver fibrosis, and hypercholesterolemia.<sup>[10]</sup> In contrast to the effect of siRNA molecules, administration of mRNA or plasmid DNA (pDNA), encoding a specific protein, could potentially lead to the (transient) overexpression of that protein.<sup>[11]</sup> In addition, administration of the genome-editing system “clustered regularly interspaced palindromic repeats” (CRISPR)/Cas9 could either lead to specific gene knockdown or to insertion of a specific gene sequence at a locus determined by the short-guide RNA (sgRNA) sequence (see Section 4.3).<sup>[12]</sup>

Over the years, a number of vehicles have been developed to enable the therapeutic application of siRNA. Several classes of

M. J. W. Evers, Dr. R. van der Meel, Dr. P. Vader, Prof. R. M. Schiffelers  
Department of Clinical Chemistry and Haematology  
University Medical Center Utrecht  
Heidelberglaan 100, 3584 CX Utrecht, The Netherlands  
E-mail: r.schiffelers@umcutrecht.nl

J. A. Kulkarni, Dr. R. van der Meel, Prof. P. R. Cullis  
Department of Biochemistry and Molecular Biology  
University of British Columbia  
Vancouver, British Columbia V6T 1Z, Canada

Dr. P. Vader  
Department of Experimental Cardiology  
University Medical Center Utrecht  
3584 CX, Utrecht, The Netherlands

 The ORCID identification number(s) for the author(s) of this article can be found under <https://doi.org/10.1002/smt.201700375>.

DOI: 10.1002/smt.201700375

nanoscale drug-delivery vehicles can be defined, such as LNPs, polymeric nanoparticles, and different types of conjugates (e.g., dynamic polyconjugates and *N*-acetylgalactosamine conjugates). Excellent reviews have been written on these vehicles and conjugates.<sup>[13–16]</sup> Here, we focus on the LNP formulations composed of four different lipid types: an ionizable amino-lipid or cationic lipid, a helper lipid, cholesterol, and a poly(ethylene glycol) (PEG)-lipid.<sup>[17]</sup> Of particular interest is the development of specialized ionizable amino-lipids that are tailored to the delivery needs of the siRNA molecule, such as intracellular trafficking to the cytoplasm, which has resulted in enhanced activity of LNP–siRNA.<sup>[18,19]</sup> At the same time, the development of rapid-mixing methods has facilitated the clinical translation and commercial success of LNPs.<sup>[2]</sup> Using rapid-mixing methods such as a staggered herringbone mixer (SHM), a uniform population of LNPs could be produced while achieving near 100% entrapment of the siRNA at small to large scale.<sup>[20,21]</sup>

A vast amount of work has been performed on the development of LNP–siRNA for therapeutic applications, and as such, here, we will focus on the design, composition, and formulation of LNP–siRNA systems with frequent references to nanoparticles encapsulating other nucleic acids such as mRNA, pDNA, and CRISPR/Cas9 components including sgRNA. We further highlight the advantages and disadvantages of various conventional and rapid-mixing production methods.

## 2. Design Principles for Lipid Nanoparticles for siRNA Delivery

### 2.1. From Liposomes to Lipid Nanoparticles

Liposomes were initially developed in the 1960s by Alec Bangham.<sup>[22]</sup> Since then, a vast amount of work has been performed to develop liposomes as drug carriers. Liposomes can act as a carrier of a wide variety of therapeutic molecules, ranging from small-molecule drugs to large proteins and nucleic acids.<sup>[23–26]</sup> They can shield therapeutic agents from degradative enzymes, improve their pharmacokinetic profile, enhance drug targeting toward specific tissues, and/or avoid tissues that are prone to side effects.<sup>[27]</sup> In the context of nucleic acids, these systems have to fulfill two roles, namely efficient entrapment of nucleic acids and intracellular delivery of the payload. We broadly define entrapment/encapsulation efficiency as the sequestration of the nucleic acids from the external environment sufficiently to protect its structure and function. Complexation efficiency only considers the ability of the vector to interact with the nucleic acid.

Initial work on neutral liposomes for the delivery of oligonucleotides was hampered by low encapsulation efficiencies.<sup>[28]</sup> With the development of cationic lipids, the charge interaction between the anionic nucleic acid and the cationic lipid improved the encapsulation of nucleic acids. Liposomes were produced using a thin-lipid-film evaporation method and an encapsulation efficiency ranging from  $\approx 30\%$  to  $40\%$  was observed.<sup>[28,29]</sup> Buyens et al. reasoned that if the cationic lipid is equally distributed among the bilayer, the encapsulation efficiency should maximally approach  $50\%$  since only half of the cationic lipid complexed with siRNA is located in the interior core of the



**Martijn J. W. Evers** received his B.Sc. in pharmacy and his M.Sc. in pharmaceutical sciences both from the University of Utrecht. In February 2017, he joined the group of Prof. Raymond M. Schiffelers at the University Medical Centre Utrecht as a graduate student working on the delivery of siRNA. His research interests include the development of both lipid nanoparticles and extracellular-vesicle-inspired drug-delivery systems for nucleic acid delivery.



**Jayesh A. Kulkarni** received his Hon. B.Sc. joint-degree in biotechnology from the University of British Columbia and British Columbia Institute of Technology. He is currently working toward his Ph.D. under the supervision of Prof. Pieter R. Cullis at University of British Columbia. His published work includes the design and development of lipid nanoparticles for intracellular delivery of DNA, and inorganic nanoparticles such as quantum dots or iron oxide nanoparticles. His main interests are the design of nanoparticle systems and their manufacturing to achieve scalability and clinical relevance.



**Raymond M. Schiffelers** is the Professor of nanomedicine at the University Medical Center Utrecht. He has over 20 years of experience in drug-delivery research. His work currently focuses on synthetic and natural nanoparticles to improve diagnosis and therapy. The work in the laboratory spans fundamental investigations on next-generation therapeutics and nanoparticles up to the final stages of nanomedicine development before first-in-man studies. One invention, OncoCort, is currently in Phase-I clinical trials.

liposome leaving the other half exposed at the surface of the liposome.<sup>[29]</sup> The presence of  $40\%$  ethanol when hydrating the lipid film with antisense oligonucleotides dissolved in citrate buffer at  $65\text{ }^{\circ}\text{C}$  resulted in an improved encapsulation efficiency of  $\approx 70\%$ .<sup>[28]</sup> A simplification of this method involved mixing lipids dissolved in ethanol with a solution of antisense

**Table 1.** Currently active clinical trials (November 2017) lipid nanoparticles/liposomes encapsulating nucleic acids.

Drug name	Nucleic acid	Disease	Phase	ClinicalTrial.gov identifier
Liposomal Grb2	Antisense oligonucleotide	Cancer	I	NCT02923986, NCT02781883, NCT01159028
MTL-CEBPA	siRNA	Cancer	I	NCT02716012
siRNA-EphA2-DOPC	siRNA	Cancer	I	NCT01591356
DCR-PH1	siRNA	Primary hyperoxaluria 1	I	NCT02795325
ARB-1467	siRNA	Chronic hepatitis B infection	II	NCT02631096
mRNA-1325	mRNA	Zika	I/II	NCT03014089
mRNA-1440/VAL-506440	mRNA	Influenza A/H10N8	I	NCT03076385
mRNA-1851	mRNA	Influenza A/H9N7	not disclosed (ND)	ND
mRNA-2416	mRNA	Cancer	I	NCT03323398
SGT-53	pDNA	Cancer		NCT02340156, NCT02354547, NCT02340117
JVRS-100	pDNA	Cancer	I	NCT00860522

oligonucleotides in citrate buffer (pH 4.0) at a ratio of 2:3 (v/v, ethanol/aqueous) at 65 °C. The resulting liposomes were large unilamellar vesicles or small multilamellar vesicles depending on the antisense oligonucleotide-to-lipid ratio used.<sup>[28]</sup> More recently, greater control was achieved over the mixing process when performed by T-junction mixing,<sup>[30–32]</sup> microfluidic mixing using an SHM,<sup>[21,33]</sup> or microfluidic hydrodynamic focusing (MHF)<sup>[34]</sup> (see Section 4). Depending on the lipid formulation, nucleic acid payload, and production method, particles containing an electron-dense core were produced for T-junction mixing and SHM with reported encapsulation efficiencies of >90%.<sup>[33,35]</sup> These observations suggested that the particle morphology was not that of a traditional liposome characterized by a lipid bilayer surrounding an aqueous core, but rather a particle characterized by an electron-dense core, referred to as LNPs (Figure 1). For LNPs, it is assumed that almost all cationic/ionizable lipid are located at the interior core of the particle, yielding high encapsulation efficiencies.<sup>[33]</sup>

Here, we define particles with a unilamellar lipid bilayer and aqueous core as liposomes, whereas particles comprising other structures are referred to as LNPs, unless particles can obviously be qualified as other well-defined structures such as cubic-phase particles. The physicochemical properties of LNPs play a profound role when dealing with barriers they encounter in the body, such as renal filtration, degradation by endonucleases, opsonization, and removal by mononuclear phagocytes, extravasation, cellular uptake, and endosomal escape.<sup>[36,37]</sup> It is therefore important to understand which physicochemical properties define the performance of LNPs and how these characteristics contribute to overcoming biological barriers for nucleic acids. In general, the following physicochemical properties of LNPs are considered to be important: lipid composition, surface properties, size, and size distribution.<sup>[14,36,37]</sup> These parameters are critical to the design and function of nanoparticles.

## 2.2. The Lipid Composition and Surface Properties of LNP–siRNA

The lipid composition of LNPs can influence particle size, particle morphology, encapsulation efficiency, and surface

properties. The most efficient LNPs used for hepatic gene silencing in the clinic contain four types of lipids: an ionizable amino-lipid (e.g., dilinoleylmethyl-4-dimethylaminobutyrate, DLin-MC3-DMA), a helper lipid (e.g., 1,2-distearoyl-*sn*-glycerol-3-phosphocholine, DSPC), a PEG lipid (e.g., 1,2-dimyristoyl-*sn*-glycerol, methoxypolyethylene glycol, PEG-DMG), and cholesterol<sup>[17]</sup> (Figure 2). The roles of these individual lipids are discussed below.

### 2.2.1. Development of Potent Ionizable Amino-Lipids

Ionizable amino-lipids are characterized by a functional group in the polar moiety of the lipid molecule with an acid-dissociation constant ( $pK_a$ ) generally below 7.0.<sup>[6,18]</sup> At physiological pH ( $\approx 7.4$ ) these lipids are largely neutral, and at acidic pH ( $< 6.0$ ) they are positively charged. Ionizable amino-lipids are designed to serve two purposes: the first is the entrapment of nucleic acids at acidic pH allowing high encapsulation efficiencies, yet at physiological pH maintaining a neutral surface charge. For *in vivo* purposes, the neutral surface charge is preferred over the use of permanently charged cationic lipids such as 1,2-dioleoyl-3-trimethylammonium-propane (DOTAP) to prevent nonspecific adsorption of negatively charged biomolecules.<sup>[38]</sup> The second role is to facilitate endosomal escape. The cationic lipid interacts with the anionic endosomal membrane, which might result in the formation of a nonbilayer hexagonal ( $H_{II}$ ) phase temporarily destabilizing the endosomal membrane leading to the release of the payload.<sup>[39,40]</sup> The most potent ionizable amino-lipids formulated in LNPs for *in vivo* applications have an apparent  $pK_a$  around 6.2–6.5, as they display an optimal balance between the neutral charge in circulation and a strong positive charge at endosomal pH.<sup>[19]</sup>

In recent years, considerable effort has been made to elucidate the relationship between the molecular structure of ionizable amino-lipids and the *in vivo* gene-silencing activity of LNP–siRNA incorporating these lipids, especially in hepatocytes.<sup>[18,19]</sup> The lipid-tail saturation, the type of linker between the lipid tail and polar head group, and the  $pK_a$  of the lipid have been found to affect hepatic gene silencing.<sup>[18,19,41]</sup> In 2005, lipids containing 2 *cis* double bonds (1,2-dilinoleyl-oxy-*N,N*-dimethyl-3-aminopropane (DLin-DMA)) showed

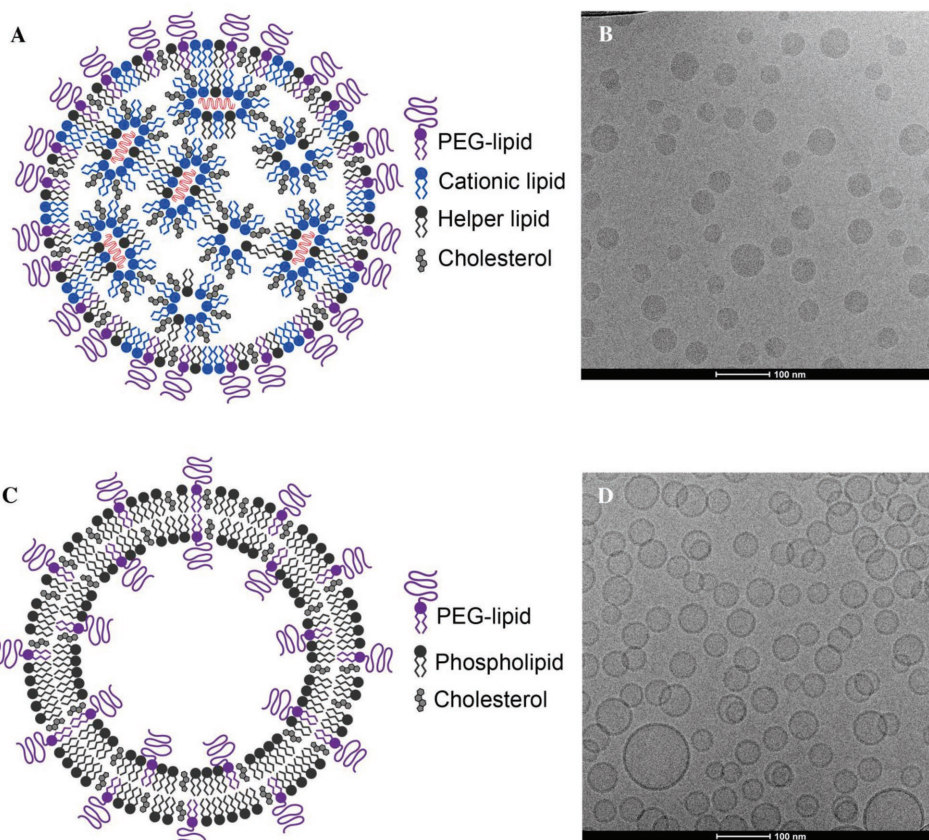


**Figure 1.** Structure of LNP-siRNA as compared to liposomes. A,B) The proposed structure of LNP-siRNA formulations containing ionizable amino-lipids within A) inverted micellar structures surrounding siRNA (in red), and B) the corresponding cryo-TEM image. The electron-dense core structure observed in the LNP-siRNA is likely to be the result of electron diffraction from lipid and nucleic acid within the particle. C,D) In contrast, liposomal formulations (depicted in panel C)) contain an aqueous core with electron densities consistent with the exterior of the liposome.

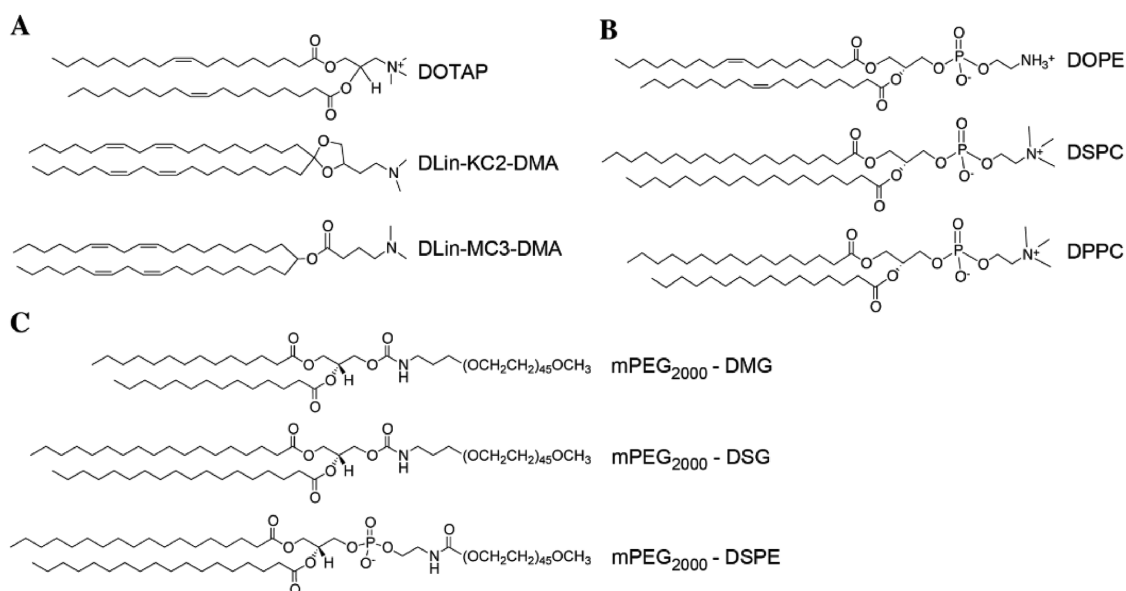


**Figure 2.** A–C) Structures of commonly reported A) cationic and ionizable amino-lipids, B) helper lipids, and C) PEGylated lipids.

improved gene silencing over lipids containing 0, 1, or 3 *cis* double bonds (1,2-distearoyloxy-*N,N*-dimethyl-3-aminopropane, 1,2-dioleoyloxy-*N,N*-dimethyl-3-aminopropane, and 1,2-dilinolenyloxy-*N,N*-dimethyl-3-aminopropane, respectively) in an in vitro model of luciferase expressing Neuro2A–G cells.<sup>[41]</sup> The underlying basis for the difference in activity was suggested to be the increased ability of the unsaturated lipid to form the inverted hexagonal ( $H_{II}$ ) phase with the anionic endosomal membrane leading to destabilization of the membrane and release of the siRNA.<sup>[39,40]</sup>

Semple et al. determined preferences within the structure of the lipid head group and linker between the lipid head group and alkyl chain.<sup>[18]</sup> Several linkers, namely ester-, alkoxy-, and ketal-linkers, between the lipid head group and alkyl chain using 1,2-dilinoleoyl-3-dimethylaminopropane (DLin-DAP), DLin-DMA, and 2,2-dilinoleyl-4-dimethylaminomethyl-[1,3]-dioxolane (DLin-K-DMA), respectively, were evaluated for in vivo silencing activity in a murine factor VII (FVII) model<sup>[42]</sup> by measuring the amount of residual FVII in serum 24 h after injection of LNP–siRNA.<sup>[18]</sup> The observed potency of the ionizable amino-lipids was DLin-K-DMA > DLin-DMA > DLin-DAP, suggesting that for these ionizable amino-lipids, incorporation of a ketal linker was superior over other linkers tested. By addition of methylene groups to the linker, it was seen that the contribution of a single methylene group (2,2-dilinoleyl-4-(2-dimethylaminoethyl)-[1,3]-dioxolane (DLin-KC2-DMA)) showed a fourfold increase in activity over DLin-K-DMA.<sup>[18]</sup> The apparent  $pK_a$  of the lipid formulated in an LNP was shown to be a critical factor for determining the potency. Of all lipids screened, the most potent formulation was based on the ionizable amino-lipid DLin-MC3-DMA with an apparent  $pK_a$  of 6.44.<sup>[19]</sup> At the same time, it was observed that optimization of the lipid formulation itself, i.e., the molar ratio between the different lipids used in the LNP influenced the observed metric for LNP potency (the effective dose to achieve 50% gene silencing or  $ED_{50}$ ). For a formulation composed of DLin-MC3-DMA/DSPC/cholesterol/PEG-lipid at 40/10/40/10 mol%, the observed  $ED_{50}$  was 0.03 mg per kg bodyweight, whereas the same formulation at 50/10/38.5/1.5 mol% had an  $ED_{50}$  of 0.005 mg per kg bodyweight.<sup>[19]</sup> The structures of several cationic and ionizable amino-lipids are shown in Figure 2 and Table 2, respectively.

Concurrently, a combinatorial-chemistry approach led to the discovery of several other lipid-like molecules (LLM) such as C12-200 and cKK-A12.<sup>[42–45]</sup> The efficacy of particles formulated with the latter lipid for hepatic gene silencing seems

to be in a similar range when compared to DLin-MC3-DMA. Similarly, Harashima and co-workers developed ionizable lipids such as YSK-05 and YSK13-C3.<sup>[46,47]</sup> The  $ED_{50}$  of siRNA against FVII formulated in a particle containing YSK13-C3/cholesterol (Chol)/PEG-DMG (68/29.1/2.9 mol%) was reported to be 0.015 mg  $kg^{-1}$  in mice.<sup>[46]</sup>

### 2.2.2. Helper Lipids and Cholesterol

1,2-Dioleoyl-*sn*-glycero-3-phosphoethanolamine (DOPE) was one of the first helper lipids used for the delivery of nucleic acids using cationic liposomes. DOPE has unsaturated acyl chains and a relatively small head group resulting in a conical shape.<sup>[14]</sup> DOPE is often referred to as a fusogenic lipid since it has the intrinsic ability to form the  $H_{II}$  phase.<sup>[48,49]</sup> The presence of DOPE in cationic lipid formulations enhances their transfection efficacy by promoting membrane fusion.<sup>[39,50–52]</sup> On the other hand, Cheng and Lee suggested it decreases the colloidal stability of particles containing DOPE designed for the delivery of siRNAs.<sup>[53]</sup>

Currently, DSPC is often used as the helper lipid in LNP–siRNA, although the functional role is not well understood.<sup>[32]</sup> DSPC has saturated acyl chains and a large head group. This results in a cylindrical geometry and strongly supports bilayer formation.<sup>[54]</sup> Thus, it is thought that DSPC stabilizes the LNP.<sup>[33]</sup> When DSPC was substituted with DOPE in formulations containing 40% ionizable lipid, the in vitro gene-silencing efficiency decreased, indicating DSPC's importance for gene-silencing activity of these particles.<sup>[55]</sup> It is remarkable that the addition of the fusogenic lipid DOPE led to a decrease in gene-silencing efficacy since, based on DOPE's fusogenic character and results obtained for other formulations containing DOPE, the opposite may have been expected. It was observed that the uptake of particles containing DOPE was decreased, although this only partly explained the difference in silencing efficacy.<sup>[55]</sup> The field would greatly benefit from enhanced insight in such observations. Additionally, computer modeling revealed that DSPC might be involved in an interaction with siRNA.<sup>[33]</sup> Increasing the amount of DSPC in an LNP–siRNA formulation from 10 to 30 mol% at the expense of the ionizable amino-lipid resulted in the formation of lamellar structures at the outer membrane layer.<sup>[56]</sup> These data indicated that a high mol% of DSPC can interfere with the inverted micellar structure observed in some LNP formulations.

**Table 2.** Characteristics of several LNPs based on cationic/ionizable amino-lipids. Lipid composition is displayed as a molar ratio of “cationic/ionizable amino-lipid”/DSPC/cholesterol/PEG-C14.

Lipid	Composition	Production method	Apparent $pK_a$	$ED_{50}$ [mg $kg^{-1}$ ]	Year of development	Author[Ref.]
DLin-DAP	40/10/40/10	Preformed vesicle method	6.2 ± 0.05	40–50	2010	Semple et al. <sup>[18]</sup>
DLin-DMA	40/10/40/10	Preformed vesicle method	6.8 ± 0.1	1	2005	Heyes et al. <sup>[41]</sup>
DLin-KC2-DMA	40/10/40/10	Preformed vesicle method	6.7 ± 0.08	0.1	2010	Semple et al. <sup>[18]</sup>
DLin-MC3-DMA	40/10/40/10	Preformed vesicle method	6.44	0.3	2012	Jayaraman et al. <sup>[19]</sup>
DLin-MC3-DMA	50/10/38.5/1.5	Preformed vesicle method	6.44	0.005	2012	Jayaraman et al. <sup>[19]</sup>
C12-200	50/10/38.5/1.5	T-junction		0.01	2010	Love et al. <sup>[44]</sup>
cKK-E12	50/10/38.5/1.5	T-junction		0.002	2014	Dong et al. <sup>[43]</sup>

Cholesterol is a major component of eukaryotic membranes.<sup>[57]</sup> Cholesterol can influence the lipid packing, membrane fluidity, and permeability of the bilayer. This has obvious implications for model membrane systems. For example, it was shown that a lipid bilayer of pure dimyristoylphosphatidylcholine in its fluid state became more condensed after incorporation of cholesterol. Incorporation of cholesterol decreased the surface area per lipid in what is known as the “condensation effect,” and this depended on the lipid formulation and temperature.<sup>[58]</sup> Moreover, as a result of a tighter lipid packing, membrane permeability was reduced.<sup>[59,60]</sup> In vivo, it was shown that cholesterol influenced the pharmacokinetics of liposomes; pure DSPC liposomes had a circulation half-life of seconds in CD-1 mice. Incorporation of 30 mol% cholesterol increased the circulation half-life of DSPC liposomes to ≈5 h. A further increase to 40 or 50 mol% cholesterol did not improve circulation half-life.<sup>[61]</sup>

Early research on the behavior of cholesterol in liposomes indicated cholesterol can exchange between lipid bilayers to equilibrate across a concentration gradient, if present.<sup>[62,63]</sup> It could therefore be reasoned that incorporation of equimolar concentrations of cholesterol, compared to endogenous membranes, would not lead to a net loss or gain of cholesterol, thereby helping to maintain particle integrity. In addition, it was also hypothesized that cholesterol restricts the diffusion of phospholipids to high-density lipoproteins in a concentration-dependent manner,<sup>[64]</sup> thereby improving particle stability in vivo. LNP-siRNAs have a hypothesized structure deviating from the typical bilayer structure. Therefore, it is questionable if the functional influences of cholesterol observed in liposomes equally apply for LNPs.

Data on the structural and functional role of cholesterol in LNP-siRNA formulations are limited. An interesting experiment by Leung et al. in 2015 showed that progressive replacement of cholesterol with DLin-KC2-DMA resulted in decreased entrapment and an increase in particle size. This observation suggested that an extremely large molar fraction of DLin-KC2-DMA inhibits the packing of lipids in a manner that supports entrapment.<sup>[56]</sup>

### 2.2.3. PEG-Lipids

An important milestone for the clinical use of LNPs in the delivery of nucleic acids is the development of PEG-lipids. PEG-lipids shield the LNP surface thereby protecting them against opsonins and uptake by the mononuclear phagocyte system, as well as preventing their aggregation in the circulation.<sup>[65]</sup> Moreover, PEG-lipids prevent aggregation during production and storage, and their incorporation can dictate LNP size.<sup>[21,66]</sup> These two functions serve to increase the overall stability of the LNP but, in doing so, potentially decrease apolipoprotein E (ApoE) adsorption to LNPs, and particle fusogenicity, both of which are paramount to achieving LNP transfection of hepatocytes.<sup>[67–70]</sup> In order to find an optimal balance in this so-called “PEG dilemma,”<sup>[71,72]</sup> a variety of “diffusible” PEG-lipids have been developed.<sup>[73,74]</sup> PEG-lipids containing shorter acyl chains (e.g., C8–14) have been found to diffuse out of the LNP more rapidly compared to the longer counterparts (e.g., C16–24) in the presence of a lipid sink (i.e., plasma lipoproteins).<sup>[69,73,74]</sup>

In 1998, a set of PEG-ceramide conjugates was developed by Webb et al.<sup>[73]</sup> It was shown that the circulation time of egg sphingomyelin/cholesterol liposomes could be tuned using different ceramide anchors attached to the PEG moiety. PEG-ceramide C20 (PEG-C20) and PEG-ceramide C24, but not PEG-ceramide C8 (PEG-C8) or PEG-ceramide C14 (PEG-C14), were found to significantly extend the circulation time of the particles. In 2005, an analogous set of PEG-diacylglycerols was synthesized, and their effect on the pharmacokinetic profiles of LNP was found to be similar to PEG-ceramides.<sup>[74]</sup> PEG-diacylglycerols were considered superior over PEG-ceramides due to the straightforward synthesis.<sup>[74]</sup> Despite longer circulation of particles with PEG-C20 or poly(ethylene glycol)-1,2-distearoyl-sn-glycero-3-phosphoethanolamine (PEG-DSPE) after a single injection, repeated administration led to an immune response leading to decreased particle circulation levels, which was not observed for PEG-C14.<sup>[75]</sup> When mice were injected weekly with liposomes, it was revealed that an increased antisense-oligonucleotides-to-lipid ratio resulted in a more severe immune response as observed after the second injection. Above a ratio of 0.08 (w/w), a rapid decrease in carrier circulation levels 1 h postinjection was observed. This immune-mediated phenomenon was not observed for PEG-C14 LNPs encapsulating antisense oligonucleotides and empty DSPC/Chol liposomes. This indicated that the presence of PEG-C20/PEG-DSPE in antisense oligonucleotide particles resulted in a rapid immune response after repeated administration.<sup>[75]</sup> Currently, PEG-diacylglycerols (PEG-DMG with C14 acyl chains) are still used as the PEG-lipid in clinical LNP-siRNA systems.

For LNP-siRNA, the dissociation of different PEG-lipids (C14, C16, and C18) from the particle was correlated to the pharmacokinetic profile and transfection efficacy of the particles.<sup>[69]</sup> The dissociation rate of the PEG-lipid from the LNP was, in particular, correlated to the length of the acyl chain. PEG-C14, -C16, and -C18 were found to desorb from the LNP in vivo at a rate of 45%, 1.3%, and 0.2% h<sup>-1</sup>, respectively.<sup>[69]</sup> Interestingly, when mice were administered with LNPs containing these PEG-lipids, the circulation half-life of the particles containing C16 and C18 acyl chain PEG-lipids was greater than particles with C14 acyl chain PEG-lipids. Within 4 h, ≈55% of the LNPs containing PEG-C14 accumulated in the liver. For LNPs containing PEG-C16 and C18, maximally 35% and 25%, respectively, accumulated in the liver and these maxima were reached at a later time point compared to PEG-C14. Not surprisingly, for extra hepatic targets such as tumors, longer circulating LNPs using PEG-C18 are used to improve tissue accumulation.<sup>[76]</sup>

When the LNPs containing different PEG-lipids were tested for hepatic gene silencing in the murine FVII model, no difference in gene silencing was observed between particles containing up to 1.5 mol% of PEG-lipid. Particles formulated with >1.5 mol% PEG-C14 retained their gene-silencing activity whereas the activity of particles containing >1.5 mol% PEG-C18 decreased. This effect was suggested to correspond with the PEG coverage; at >1.5% of PEG, the surface of the LNP is fully covered with PEG, whereas at 1.5 mol% and lower, this is not the case.<sup>[69]</sup> When >1.5% PEG is used, the more rapid dissociation of PEG-C14 ensures that the surface is exposed more readily than when C18 is used. When the surface of a

particle containing ionizable amino-lipids is gradually exposed, it is opsonized by ApoE. Subsequent uptake of the particle is mediated by ApoE-dependent uptake via the low-density lipoprotein receptor.<sup>[70]</sup> The importance of ApoE adsorption for the efficacy of LNPs containing an ionizable lipid was illustrated using ApoE knockout mice (ApoE<sup>-/-</sup>). When LNPs encapsulating an siRNA against FVII were administered to both wild type (WT) and ApoE<sup>-/-</sup> mice, the gene silencing was attenuated in the latter. When LNPs were preincubated with various concentrations of ApoE, the gene-silencing activity was rescued in an ApoE dose-dependent manner.<sup>[70]</sup> The opposite was observed for particles designed for tumor accumulation. Increasing the amount of PEG-C18 from 2.5 to 5.0 mol% resulted in elongated circulation times and an increased accumulation in tumor tissue.<sup>[76]</sup> This highlights how, by altering the PEG anchor and density, LNP pharmacokinetics and tissue distribution may be tuned for specific applications.

### 2.3. Nitrogen-to-Phosphate (N/P) Ratio

An important aspect of LNP-siRNA design is the ratio of elemental nitrogen and phosphate (N/P ratio). This ratio describes the charge interaction between the cationic charge of the amino (N<sup>+</sup>) group in the ionizable amino-lipid to the anionic charge of the phosphate (PO<sub>4</sub><sup>-</sup>) groups in the backbone of nucleic acids and is the basis of the complexation of siRNA with the ionizable amino-lipid. Patisiran is generated at N/P = 3 with 1.5 mol% PEG-lipid (resulting in a particle size of ≈50 nm). When 30 nm LNP-siRNA containing 50 mol% of the ionizable amino-lipid 3-(dimethylamino)propyl(12Z,15Z)-3-[(9Z,12Z)-octadeca-9,12-dien-1-yl]henicosa-12,15-dienoate and 5 mol% PEG-DMG were formulated at N/P ratios of 1–12, modest changes to the N/P (up to 6) improved the achieved ED<sub>50</sub> from 1.15 mg kg<sup>-1</sup> at N/P = 1 to 0.45. At higher N/P values, no further improvement in gene silencing was observed.<sup>[66]</sup> Chen et al. suggested that this was an indication that additional ionizable amino-lipids, which do not interact with the encapsulated siRNA, should be available to enhance endosomal escape.<sup>[66]</sup>

### 2.4. Size

Size is regarded as an important physicochemical parameter that affects the in vivo behavior of LNPs.<sup>[36,37]</sup> LNP diameter size, here, is displayed as a Z-average measured by dynamic light scattering (DLS), unless stated otherwise. Size influences the pharmacokinetic profile of LNPs, as smaller particles display longer circulation times and slower clearance from the bloodstream.<sup>[77]</sup> Previous reports on CD-1 mice have indicated that LNP size for hepatic gene silencing should be limited to sub-100 nm particles since these nanoparticles can readily pass the liver fenestrae, enter the space of Disse, and interact with hepatocytes.<sup>[66,78]</sup>

The development of rapid-mixing methods has improved the ability to produce homogeneous particles, thereby enabling the study of particle size on pharmacokinetic behavior as size distributions are more uniform.<sup>[20,21,33,79]</sup> Andar et al. were

able to produce relatively monodisperse liposome populations of ≈40 nm, ≈72 nm, ≈98 nm, ≈162 nm, and ≈277 nm without overlapping size distributions as measured by asymmetric flow field-flow fractionation (AF<sup>4</sup>) in line with multiangle laser light scattering and quasi-electric light scattering (QELS).<sup>[79]</sup> It was shown that uptake of 1,2-dipalmitoyl-sn-glycero-3-phosphocholine (DPPC)/cholesterol/dipalmitoylphosphatidylethanolamine-PEG2000 (50/40/10 mol%) liposomes by Caco-2 cells showed size-dependent trends, whereby the cells favored smaller (≈40 nm) over larger particles (>98 nm). Although these experiments were not performed using LNP-siRNA, these data illustrate that particle uptake can be influenced by size. Moreover, the endocytic processing differed based on particle size. Endocytosis of 40 nm LNPs was shown to be mainly dynamin dependent, whereas particles larger than 98 nm were influenced mainly by the clathrin-dependent pathway,<sup>[79]</sup> although it must be noted that clathrin-dependent endocytosis also critically depends on dynamin,<sup>[80]</sup> making it difficult to draw strong conclusions from these observations. The uptake mechanism is of importance as the intracellular processing of nanoparticles can be influenced by the uptake pathway.<sup>[81–83]</sup> For LNP-siRNA containing the ionizable lipid DLin-MC3-DMA, two uptake pathways have been shown to be active: clathrin-mediated endocytosis and macropinocytosis. It was observed that the majority of the gene-silencing effect resulted from particles taken up via macropinocytosis.<sup>[83]</sup> This indicates that the route of uptake has consequences for the efficacy of LNPs. Moreover, as shown for LNP-siRNA, the escape of siRNA to the cytoplasm only occurred at a low rate and in a specific part of a cellular trafficking pathway.<sup>[83,84]</sup>

The hepatic gene silencing of FVII in mice using 27, 38, 43, 78, and 117 nm sized LNP-siRNAs (as measured by DLS, number-weighted) was investigated by Chen et al.<sup>[66]</sup> The gene silencing of FVII was strongly dependent on particle size. The hepatic gene silencing of 38–78 nm sized particles was far more efficient compared to particles of 117 or 27 nm with the 78 nm sized particles showing maximal gene silencing. It was suggested that the large 117 nm particles were unable to pass through the fenestrations (≈100 nm) in the liver vasculature, resulting in a less potent formulation. For the smaller 27 nm particles, the decrease in efficacy was shown to correlate to a decreased particle stability in serum. When the pharmacokinetic profiles of 27, 43, and 78 nm particles were evaluated, liver accumulation was substantially affected by size, favoring smaller 27 and 43 nm particles over 80 nm particles.<sup>[66]</sup> In addition, the size-dependent stability of nanoparticles influenced the in vivo efficacy of the nanoparticles. In smaller LNPs, the ionizable amino-lipid more rapidly dissociated from the particles, resulting in lower gene-silencing efficiency. When smaller particles (e.g., 27 nm) were formulated at a higher N/P ratio of 6, improvements in transfection efficacy were seen compared to particles formulated at an N/P ratio of <3. The decrease in gene-silencing potency of smaller particles (27 nm) could not solely be ascribed to a decreased content of ionizable amino-lipid.<sup>[66]</sup> A major confounding factor in this study could be the amount of PEG-DMG lipid in the particle. The size of the particles was tuned by varying the amount of PEG-lipid within a particle. Particles of 30 nm contained ≈5 mol% PEG-DMG whereas particles of 80 nm contained ≈0.5 mol% PEG-DMG. It is known that these LNPs are taken up via ApoE-dependent

endocytosis and that PEGylation prevents ApoE from binding to the particle, thereby possibly influencing the gene silencing. An additional explanation could be the decreased siRNA payload per particle for the 30 nm particle compared to the 80 nm particle.<sup>[66]</sup>

Taken together, these studies show the impact of various design parameters, such as lipid composition and size, on LNP–siRNA pharmacokinetics and (hepatic) gene-silencing efficacy. Future research could be aimed at reaching targets beyond the liver by exploiting the multitude of possibilities offered by the LNP platform.

### 3. Production of Liposomes and Lipid Nanoparticles

Liposomes and LNPs can be produced using several methods. First, we shortly discuss the characteristics of the most commonly reported conventional ones: lipid-film hydration followed by extrusion, sonication, or homogenization methods, and ethanol injection. For in-depth information on these, the reader is referred to reviews and excellent book chapters written on (conventional) liposome production.<sup>[85–89]</sup> Second, we describe three more recent methods based on the principle of the ethanol-injection method: in-line T-tube mixing, MHF, and SHM.

#### 3.1. Conventional Methods for the Production of Liposomes

##### 3.1.1. Thin-Film Hydration and Size-Reduction Techniques

The thin-film hydration method is a common manufacturing method for the production of liposomes and is considered a top-down approach where large lipid vesicles are re-formed to small vesicles using high-energy size-reduction methods.<sup>[85]</sup> Lipids are dissolved in an organic solvent (e.g., chloroform) and transferred to a steel production vessel or a round-bottom flask. The organic solvent is removed in vacuo resulting in a lipid film on the surface of the vessel or flask. Upon hydration with an aqueous solution, large multilamellar vesicles are formed. This population of vesicles is very heterogeneous and the size distribution is centered around several micrometers in size.<sup>[85,88]</sup> Size-reduction steps, such as extrusion or sonication, are generally used to generate small unilamellar vesicles. Extrusion is the process of repeatedly forcing a heterogeneous suspension of particles through a polycarbonate or inorganic filter of a designated pore size (e.g., 0.1  $\mu\text{m}$ ). This results in a population of unilamellar vesicles, with sizes in the range of the size of the pores.<sup>[85,90]</sup> Sonication is an alternative method to reduce particle size using a probe sonicator or a bath sonicator. For probe sonication, the tip is placed in a dispersion of multilamellar vesicles.<sup>[88,91,92]</sup> The size of the particles after sonication depends on the lipid composition and the time of sonication, although sonication offers significantly less control over the resulting size than processes such as extrusion.<sup>[89]</sup> An additional method for size reduction, mostly used for larger batches, is high-pressure homogenization. Particles can be homogenized using

different machines, such as high-pressure machines with a ring shaped gap valve (e.g., French pressure cell) or with an interaction chamber where two fluids collide (microfluidization).<sup>[88,93]</sup> In microfluidization, the liposomal suspension is pumped at high velocity through an inlet that is divided into two streams and progressively bifurcates. These streams eventually collide within an interaction chamber leading to the formation of smaller particles due to extreme conditions of turbulence and pressure.<sup>[91,93]</sup>

Liposomes containing siRNA have been prepared using the lipid-film method and subsequent postprocessing method such as extrusion and sonication. For example, cationic lipoplexes produced using thin-film hydration and subsequent bath sonication yielded particles with a size of 196 nm.<sup>[94]</sup> Additionally, liposomes were produced by hydrating a lipid film of DOTAP/DOPE/DSPE-PEG (47.5/47.5/5 mol%) with a solution of siRNA in 4-(2-hydroxyethyl)-1-piperazineethanesulfonic acid (HEPES) resulting in particles ranging between  $\approx 80$  nm and  $\approx 300$  nm and an encapsulation efficiency of  $\approx 43\%$ .<sup>[29]</sup> For liposomes prepared using the thin-film method, encapsulation efficiencies generally approach  $\approx 50\%$ .<sup>[29,95]</sup> It was shown by Semple et al. that the addition of 40% of ethanol during lipid-film hydration improved the encapsulation efficiency of pDNA to 70%.<sup>[28]</sup> This method could be simplified by mixing preheated solutions of lipids in ethanol and oligonucleotides in buffer and subsequent dialysis. This method is referred to as the preformed vesicle method.<sup>[28]</sup> As a result, a mixed population of small (80–140 nm, measured by freeze–fracture electron microscopy and QELS) uni- and multilamellar vesicles was formed.

##### 3.1.2. Ethanol-Injection Method

The ethanol-injection method was first described by Batzri and Korn and was developed as an improved alternative to the thin-film hydration method combined with sonication, which has several drawbacks (see Section 4.2).<sup>[96]</sup> A solution of lipids in ethanol was injected via a syringe to a solution of KCl diluting the ethanol to a concentration of 7.5% (v/v). A relatively homogeneous solution of particles was formed with an average size of  $\approx 27$  nm (measured by electron microscopy). This size approached the smallest size achievable for a liposome of composition phosphatidylcholine/stearylamine (91.25/8.75 mol%). When the ethanol was quickly diluted in the aqueous buffer, lipid vesicles self-assembled due to a rise in solvent polarity.<sup>[96]</sup>

The crossflow injection method was developed as an alternative to the ethanol-injection method, since the latter method was confined to the batch production of low-lipid-concentration products, and reproducibility between batches was considered improvable.<sup>[97]</sup> This system contained a crossflow module where two stainless-steel tubes were welded perpendicular to one another, and a small injection hole was present at the intersection between the tubes. Through this injection hole, ethanol containing lipids could be injected into a stream of aqueous buffer resulting in the formation of liposomes. Liposome size could be influenced by several parameters; at higher flow rates of the aqueous buffer streams, smaller-sized particles were obtained. In addition, at higher injection pressures of the ethanol solution containing lipids, the resulting particles were found to be smaller.<sup>[97]</sup>

### 3.2. Drawbacks of Conventional Production Methods

Currently, these “conventional” methods of lipid-film hydration and ethanol injection are still widely used for the production of nanoparticles. However, the labor-intensive processes, the lack of scalability, and the reproducibility of certain steps have been cited as the major drawbacks of these techniques.<sup>[85]</sup>

The thin-film hydration method is a labor-intensive, multi-staged manufacturing method that is costly and difficult to scale up.<sup>[85,98–100]</sup> The multiple steps of the thin-film hydration method, including evaporation of organic solvent, extrusion of large volumes of liposomes, and possibly passive loading of liposomes, are time consuming at a large scale. For example, evaporation of organic solvent might take multiple hours at large volumes.<sup>[85]</sup> Additionally, most size-reduction methods are prone to scalability issues; extruding large volumes of lipid vesicles might result in clogging of the membrane leading to product losses,<sup>[98]</sup> although a simple solution is to determine the maximum achievable lipid per surface area of membrane, and set an operating threshold below this number. Sonication is also very difficult to scale up.<sup>[20,101]</sup> Microfluidization is a method to produce liposomes at a large scale, but the high pressure during this process can cause shear stress and may be harmful to labile compounds. The potential for channel blocking may also exist.<sup>[87]</sup> Furthermore, the transition from a lab-scale production of liposomes to a clinical-scale production is reported to be challenging since physicochemical properties might vary when batches are produced at larger scale.<sup>[102,103]</sup>

Regarding reproducibility within a large production vessel, manufacturing conditions might vary within and between batches resulting in variability and heterogeneity.<sup>[104]</sup> Even when producing small batches, the relative size of the round-bottom flask compared to the size of the particles is several orders of magnitude. This discrepancy might lead to local hydration conditions, which are nonuniform at the scale of a liposome, and variability in the interliposomal composition, even when produced at the laboratory scale.<sup>[104,105]</sup> Specific methods have been established to deal with the heterogeneity in the case of lipid-film hydration. For example, extrusion is reported to give quite reproducible results although it introduces an additional manufacturing step.<sup>[106]</sup> For the ethanol-injection method, at a stirred batch scale, reproducibility is also difficult to achieve.<sup>[97]</sup> The improved crossflow injection method may provide a well-defined, controllable and reproducible alternative.<sup>[97]</sup>

Sample contamination and degradation have also been reported to be potential issues for some of the methods mentioned above. For example, sonication can lead to oxidation and degradation of lipids or the drug content, as well as to local overheating of the sample. Probe sonication has been shown to leach titanium particles into the product.<sup>[96,107]</sup>

Furthermore, it is important to mention that when nanoparticles are produced for *in vivo* applications (i.e., parenteral administration), sterile aseptic technique/maintenance of sterility is critical in commercial-scale processes. Sterile filtration after production using a 0.2  $\mu\text{m}$  membrane is a very straightforward and convenient method for the sterilization of small (<200 nm) liposomes/LNPs but does not remove toxins. If this is not a possibility due to particle size,

the entire manufacturing process would have to be sterile, which is more complex and expensive compared to sterile filtration.<sup>[88]</sup>

Entrapment of hydrophilic drugs into liposomes by passive-loading techniques generally yields a low encapsulation efficiency. This can be partly circumvented by active-loading techniques as reported for amphipathic molecules (remote loading) or for nucleic acids (complexation with ionizable amino or cationic lipids).<sup>[108]</sup> However, remote loading is certainly not applicable to all drugs and mostly suitable for amphipathic molecules.<sup>[109]</sup> Addition of ethanol during lipid-film hydration leads to improved encapsulation efficiencies for nucleic acids. However, this method depends on adequate mixing of ethanol and water, and methods such as ethanol injection or the pre-formed vesicle method do not provide adequate control over the mixing process, resulting in suboptimal formulations.<sup>[85,97]</sup>

Nevertheless, despite the mentioned drawbacks, conventional methods for the production of liposomes/LNPs remain popular, as they are easy to implement<sup>[110]</sup> and execute at a laboratory scale and not necessarily hamper large-scale production, evidenced by approved liposomal products such as Doxil<sup>®</sup>. The necessary equipment is relatively inexpensive, making these methods widely accessible.<sup>[86,111]</sup> However, it should be emphasized that a lack of scalability is one of multiple causes for the lack of clinical translation of nanomedicine.<sup>[112]</sup> To address this issue, the European Union has funded several initiatives, including The European Pilot Line for good manufacturing practice manufacturing of batches for clinical trials and the European Nanomedicine Characterization Laboratory, where promising nanomedicines can be developed while fully taking into account downstream considerations. Therefore, the development and implementation of new production methods that deal with the issue of scalability may be of utmost importance for the clinical success of nanomedicine. New production methods based on rapid mixing of ethanol and water to encapsulate nucleic acids have the characteristics to deal with these issues of reproducibility, scalability of production, and encapsulation efficiency.

### 3.3. New Production Methods for Lipid Nanoparticles

Several improved strategies based on the ethanol-injection method have been developed more recently. In-line T-junction mixing has been used to mix an organic and aqueous phase in a controlled manner for the production of LNP–pDNA and LNP–siRNA.<sup>[30–32]</sup> Alternatively, two microfluidic methods have been redesigned for the production of LNPs: MHF<sup>[34]</sup> and SHM.<sup>[21,33]</sup> Microfluidic mixers can be differentiated based on an active or passive type of mixer. For example, the flow of liquids can be actively influenced by electro-hydrodynamic disturbances, whereas in passive mixers, the geometry of the microfluidic chip is used to increase the interface between two fluids to improve the mixing.<sup>[113]</sup> Both MHF and SHM are passive microfluidic mixers.

The three aforementioned rapid-mixing methods differ in the 3D structure of the devices, but they all possess the ability to induce rapid mixing of an organic and an aqueous phase in a controlled environment. The general principle of LNP production is therefore the same. LNPs are formed by a quick increase

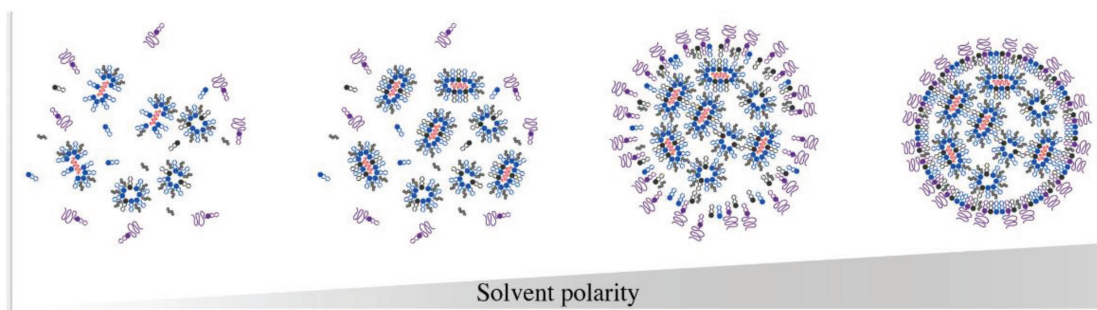


**Figure 3.** Increase in solvent polarity drives the self-assembly of LNP–siRNA formulations. LNP–siRNA are hypothesized to form an electron-dense core structure as a result of significant lipid and nucleic acid present in the internal compartment. The first interactions to occur, upon mixing of the ethanol and aqueous streams, are those between cationic lipids and negatively charged nucleic acids. As the solvent polarity progressively increases, the hydrophobic inverted micellar structures coalesce, generating the core of the LNP. As mixing continues, more polar lipids (such as PEG-lipid and DSPC) coat the surface of the nanoprecipitates. The resulting part has an electron-dense core structure surrounded by a lipid monolayer.

in polarity of the environment induced by rapid mixing of the two miscible phases. This rapid mixing induces supersaturation of lipid molecules which leads to the self-assembly of LNPs (**Figure 3**). In this regard, these production methods are considered bottom-up approaches since LNPs self-assemble into the desired structure without the need for size-reduction methods. The main benefits of rapid-mixing processes over conventional methods for LNP production are the enhanced control of physicochemical properties,<sup>[114]</sup> improved encapsulation efficiencies, and an improved ability to scale up.

### 3.3.1. T-Junction Mixing

The use of T-junction mixing in lipid-based drug delivery was first described in 1999 by Hirota et al. as a method for the production of DNA–lipoplexes, providing an alternative to macroscopic mixing methods.<sup>[115]</sup> The T-junction mixer provided a controlled mixing environment compared to macroscopic mixing methods (e.g., vortexing or pipetting), leading to reproducible production of lipoplexes.<sup>[115,116]</sup> The rapid mixing occurred when the two input streams in the T-junction collided, resulting in a turbulent output flow (**Figure 4**).<sup>[117]</sup> This production method has also been applied to the production of LNP–siRNA.<sup>[30,35,41,118]</sup> The mechanism of LNP formation was based on the precipitation of lipids as the solvent polarity increased upon dilution of the ethanolic phase into the aqueous phase.<sup>[119]</sup> Unfortunately, limited data are available on the influence of operating controls such as flow and flow-rate ratio (FRR) on the polydispersity index (PDI) and particle size of LNP–siRNA. However, the effect of these variables might be illustrated using data from the production of LNPs containing a hydrophobic core of triolein encapsulating iron oxide nanoparticles. For these systems, increasing flow rates resulted in smaller particle size. At a flow rate of 10 mL min<sup>-1</sup>, particles sizes were found to be 75 ± 6 nm, whereas at a flow rate of 40 mL min<sup>-1</sup> much smaller particles were formed (36 ± 2 nm) (cryo-transmission electron microscopy (TEM) and DLS, number weighted). At lower flow rates, the PDI was higher compared to higher flow rates indicating how particle characteristics could be tuned using the flow rate.<sup>[117]</sup>

Relatively few siRNA- and DNA-loaded nanoparticles have been produced at a laboratory scale using T-junction mixing, although some knowledge has been obtained on particle size, morphology, and encapsulation efficiency. Jeffs et al. used a T-junction with a diameter of 1.6 mm to mix a solution of lipids in ethanol and pDNA dissolved in Tris-ethylenediaminetetraacetic acid-buffer at a flow rate of 1 mL s<sup>-1</sup> in order to produce liposomes.<sup>[31]</sup> T-junction mixing was used to stepwise dilute the ethanol content. Two consecutive passages through the T-junction system were applied, diluting the ethanol content: first from 100% to 45% (v/v) then from 45% to 22.5% (v/v). The resulting particles were 116 ± 54 nm in size (QELS, volume-weighted) and the encapsulation efficiency was 74%. When a single ethanol-dilution step to 22.5% (v/v) was performed, the encapsulation efficiency dropped to 17%. A combination of uni- and multilamellar vesicles was observed.<sup>[31]</sup> A similar T-junction

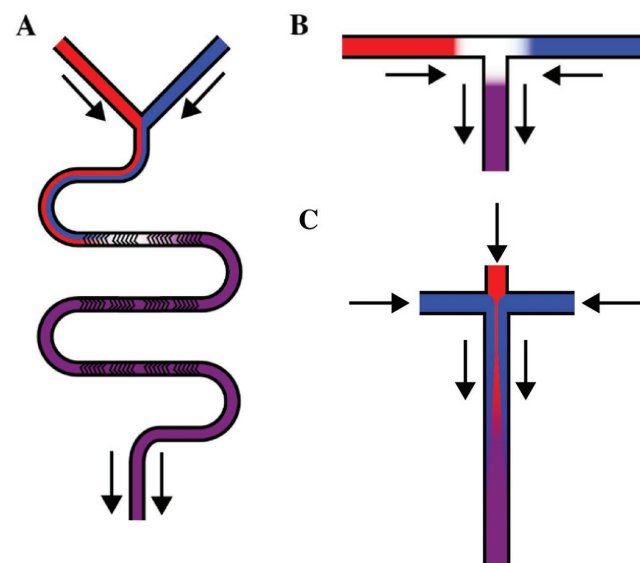


**Figure 4.** A–C) Schematic illustration of new mixing methods: microfluidic mixing using A) a staggered herringbone mixer, B) in-line T-junction mixing, and C) microfluidic hydrodynamic mixing. The aqueous phase is illustrated in blue, the organic phase in red, and the resulting mixture containing particles in purple.

mixing setup was used for the production of LNP–siRNA (DLin-DMA/DSPC/Chol/PEG-c-DMA; 30/20/48/2 mol%). The resulting particles were found to be  $140 \pm 6$  nm in size (PDI of 0.11).<sup>[41]</sup> Similarly, an adaptation to the protocol of Jeffs et al. was used by Abrams et al. who produced particles (CLinDMA/cholesterol/PEG-DMG, 50/44/6 mol%) using a T-junction mixer at a flow rate of  $40 \text{ mL min}^{-1}$  diluting the ethanol in a single step.<sup>[30]</sup> The resulting particles were 140 nm and the encapsulation efficiency was 82%. Crawford et al. showed that LNP size and morphology are influenced by the lipid composition of the particles.<sup>[35]</sup> When the mol% of PEG-DMG was increased (while at the same time decreasing the mol% of cholesterol), a decrease in size was observed: particles containing 2 mol% PEG-DMG were 120 nm (PDI of 0.075), whereas particles containing 5.4 mol% PEG-DMG were 63 nm (PDI of 0.083). In addition, the morphology of the particles containing 2 mol% was considered to be more spherical compared to particles containing 5.4 mol% PEG-DMG.<sup>[35]</sup>

Together, these results suggest that LNP–siRNA can be produced using T-junction mixing. Encapsulation efficiencies are generally higher as compared to conventional methods. However, the use of this method at the laboratory scale is limited due to the high flow rates required to ensure rapid mixing, which can be difficult to reconcile with small laboratory-scale batches.<sup>[119]</sup> Nevertheless, in-line T-junction mixing is the preferred method of production on a large scale by companies engaged in the production of LNP–siRNA.<sup>[55]</sup>

An alternative to the setup of conventional T-junction mixers can be the use of microfluidic T-shaped designs. In these microfluidic designs, solutions experience laminar flow, and mixing is then characterized by diffusion, which is relatively slow.<sup>[120,121]</sup> In diffusional mixing, the degree of mixing is dependent on the length of the channel and the contact surface area of the two streams.<sup>[122]</sup> At higher Reynolds numbers, caused by higher flow rates, chaotic flows lead to improved mixing efficiencies.<sup>[120]</sup> Shorter mixing times lead to a decreased influence of mass-transport effects, which are known to cause lipid aggregation and heterogeneous particle populations.<sup>[20]</sup> Stroock et al. have shown that addition of herringbone-like structures improves the mixing of a Y-shaped channel at low Reynolds numbers, thereby making it possible to ensure rapid millisecond mixing at lower flow rates.<sup>[122]</sup> This offers the opportunity to prepare smaller-scale batches and may therefore be preferred over T-junction mixing designs.<sup>[119]</sup>

### 3.3.2. Microfluidic Hydrodynamic Focusing

MHF is a microfluidic-mixing technique<sup>[123]</sup> used to manufacture liposomes in a reproducible and scalable fashion.<sup>[104]</sup> MHF is a continuous-flow technique where, in the case of liposome production, lipids dissolved in an organic solvent are hydrodynamically focused using an aqueous phase (Figure 4). This technique, applied for the production of liposomes, was extensively investigated between 2004 and 2010 by Jahn et al.<sup>[104,124]</sup>

The flow within the system is characterized as laminar. These laminar conditions result in a well-defined interface

between the organic and aqueous phases where interfacial forces dominate. By influencing this interface using the operating parameters, the operator can gain control of the size and PDI.<sup>[104]</sup>

The operating parameters of this system were found to be the total flow rate of both phases (volume/time) and the ratio in flow rates between the aqueous and organic phases, which influenced the degree of hydrodynamic focusing (i.e., width of the center stream).<sup>[104,124]</sup> Moreover, the influence of these two variables on particle size and polydispersity index varied with different microfluidic channel geometries. The basis of nanoparticle formation in MHF was a decrease in lipid solubility at the interface between the organic solvent and water. At a critical level, it was energetically favorable for the lipid to first form disk-like shapes and then close into a confined spherical form.<sup>[104,124,125]</sup> The size and size distribution of the nanoparticles were dependent on the characteristics of the diffusion, which in turn were influenced by the degree of hydrodynamic focusing.<sup>[124,126]</sup> A higher FRR (aqueous-to-organic flow rate) resulted in smaller particles with a narrower size distribution. Increasing the total flow rate resulted in larger particles at low FRRs. At high FRRs, this effect was negligible. Additionally, the microfluidic chip geometry had an influence on the operating variables FRR and flow rate. When the diameter of the channel was reduced from 65 to 10  $\mu\text{m}$ , equally sized particles were obtained at a twofold lower FRR.<sup>[124]</sup>

*Flow Rate and Ratio Determine Particle Size by Influencing Mixing:* The influence of flow rate and FRR on particle size might be explained by their effect on the process of particle formation during MHF. Mixing in the MHF setup was found to be either diffusive mixing or convective–diffusive mixing, wherein the latter induced faster mixing.<sup>[124]</sup> Convective–diffusive mixing occurred in the focusing region, whereas diffusive mixing was present in the downstream mixing channel. Rapid convective–diffusive mixing of ethanol and buffer led to the formation of small particles with a narrow size distribution, whereas slow diffusive mixing led to larger particles with broader size distributions.<sup>[124]</sup> The total flow rate and the degree of hydrodynamic focusing influenced the ratio between particle formation in the convective–diffusive versus the diffusive regions, thereby affecting particle sizes and size distributions. High focusing occurred at a high FRR, shifting particle formation toward the convective–diffusive region and reducing particle size, whereas low focusing resulted in a broader center stream enhancing diffusive particle formation, thereby increasing particle size and size distribution.<sup>[124]</sup>

Krzysztoń et al. used a similarly shaped device as Jahn et al. to produce siRNA-loaded “monomolecular nucleic acid/lipid particles.”<sup>[34]</sup> Using this method, small liposomes ( $\approx 20$  nm, measured using fluorescence correlation spectroscopy) consisting of DOTAP/DOPE/1,2-dioleoyl-sn-glycero-3-phosphocholine (DOPC)/DSPE-PEG2000 (8.2/41/41/8.2/1.6 mol%) could be produced encapsulating  $\approx 70\%$  of 21 bp dsDNA at an N/P of 6.<sup>[34]</sup> Hood and DeVoe noted that the low flow rates of MHF limit the scale-up opportunities, and developed a vertical flow-focusing device (VFF) producing  $100 \text{ mg h}^{-1}$  liposomes at a flow rate of  $4.5 \text{ mL min}^{-1}$ .<sup>[99,127]</sup> Nevertheless, the use of MHF for the production of LNP–siRNA has therefore been limited.

### 3.3.3. Staggered Herringbone Mixing

Microfluidic mixing by chaotic advection using an SHM for the production of LNPs was pioneered by the group of Pieter Cullis and subsequently commercialized by Precision Nano-systems.<sup>[20]</sup> This method was developed in order to improve the control over the mixing process and shorten the mixing time.<sup>[2,21]</sup> Similar to other microfluidic techniques, the main characteristic is controlled millisecond mixing of two miscible phases, usually ethanol and an aqueous buffer. The structure of the staggered herringbone mixer allows efficient wrapping of the two fluids around each other resulting in an exponential enlargement of the interface between the fluids ensuring rapid mixing<sup>[122]</sup> (Figure 4). The sudden, rapid increase in polarity of the environment of lipid molecules leads to supersaturation, and is thought to result in the formation of LNPs.<sup>[21,105]</sup> The particle size and size distribution have been found to be controlled by the total flow rate and the FRR.<sup>[20,21,128]</sup> For commercial instruments, such as the NanoAssemblr, the geometry of the microfluidic method is predetermined. Therefore, size and size distribution cannot be influenced by microfluidic chip design. It was found that parameters that could be varied, such as lipid composition and payload, influenced the size and morphology of LNPs.<sup>[20,21,32,56]</sup> LNP production using the SHM can be readily scaled up by parallelization of microfluidic chips.<sup>[21,100]</sup>

*Operating Parameters Influence Particle Characteristics:* Zhigaltsev et al. postulated that the increase in polarity is determined by two factors: “the rate of mixing and the ratio of aqueous to ethanol volumes that are being mixed.”<sup>[20]</sup> The rate of mixing was observed to be determined by the total flow rate. The same rationale was applied to the ratio between the volumes. A larger difference in volume between the two fluids resulted in faster mixing and an increased dilution effect.<sup>[20]</sup> For electron-dense LNP–siRNAs consisting of DLin-KC2-DMA/DSPC/cholesterol/PEG-c-DMA (40.0/11.5/47.5/1.0 mol%), it was seen that at flow rates of  $>0.2 \text{ mL min}^{-1}$ , particle size remained constant at  $\approx 55 \text{ nm}$  with a low ( $<0.1$ ) PDI (DLS, number weighted).<sup>[21]</sup> The encapsulation efficiency was  $>95\%$ . Flow rates below  $0.2 \text{ mL min}^{-1}$  resulted in larger, more polydisperse sized samples (PDI  $> 0.1$ ) indicating suboptimal mixing. Therefore, it seemed that above a certain threshold flow rate, particles remained equally sized, whereas below this threshold, particle size and polydispersity index increased.<sup>[21]</sup> This may have resulted from increased mixing times at low velocities. Increased mixing times might have caused pockets of ethanol which led to the growth of larger intermediate structures and subsequently larger LNPs.<sup>[129]</sup>

The FRR generally shows an inverse relationship with particle size, i.e., an increase in FRR leads to a smaller particle size with a low ( $<0.2$ ) PDI as a result of decreased mixing time.<sup>[20,21]</sup> For DOTAP/DOPE (50:50 mol%) liposomes, it was observed that an increase in FRR resulted in smaller particles as expected, although the PDI increased. At a flow rate ratio of 5:1 (aqueous/ethanol) and a flow rate of  $2.0 \text{ mL min}^{-1}$ , the resulting particle population showed a PDI of 0.4.<sup>[130]</sup> However, compared to the LNP–siRNA produced by Belliveau et al., which were  $55 \text{ nm}$  with a PDI of  $<0.1$  at flow rates of  $>0.2 \text{ mL min}^{-1}$ , these particles were much more polydisperse.<sup>[21,130]</sup> In general,

an increasing FRR or flow rate is suggested to lead to rapid-mixing rates so that particles will adopt a minimal size based on the lipid constituents.<sup>[131]</sup> The high PDI (0.4) of these DOTAP/DOPE liposomes may indicate that a combination of DOTAP/DOPE might not result in a stable liposomal system.

*Limit-Size Concept:* The limit-size concept, as set out by Zhigaltsev et al., suggests that when particles are produced using SHM under rapid-mixing conditions, they adapt the smallest thermodynamically stable size based on the physical properties of lipids and the specific lipid composition of the particle.<sup>[20]</sup> The basis of the limit-size calculations is the packing properties of the combination of lipids based on their physical properties. Belliveau et al. reasoned that if sublimit particles are formed during the manufacturing process, these particles ultimately coalesce to form particles determined by the physical constraints of the lipid components.<sup>[21]</sup> Given this reasoning, changes in lipid composition would result in different particle sizes. This has been shown for particles containing different amounts of PEGylated lipid, 1-palmitoyl-2-oleoyl-sn-glycero-3-phosphocholine (POPC)/cholesterol, and POPC/triolein.<sup>[20,21,131]</sup>

*Morphological Differences among LNPs Produced by SHM:* The lipid constituents do not only determine LNP size but also morphology. When LNP–siRNA were produced using SHM, two different morphologies could be distinguished based on cryo-TEM images:<sup>[56]</sup> particles containing an electron-dense core and (multi)-lamellar nanoparticles. Differences in morphology were attributed to differences in lipid composition and the interplay with the nucleic acid payload.<sup>[56]</sup>

LNP–siRNA were also observed as having an electron-dense core structure by Leung et al.<sup>[33]</sup> Using cryo-TEM and in silico simulations, it was shown that in the presence and absence of siRNA, LNPs containing DLin-KC2-DMA/DSPC/cholesterol/PEG-c-DMA (40/11.5/47.5/1 mol%) had an electron-dense core. This core was hypothesized to consist of inverted micelles of ionizable amino-lipid complexed with or without siRNA<sup>[33]</sup> (Figure 1A). Upon mixing in an SHM, the relatively hydrophobic complexes of siRNA and ionizable amino-lipid precipitate out of solution and act as nucleation point.<sup>[21,33]</sup> Subsequently, these inverted micelles are coated with a layer of polar lipids such as DSPC and PEG-lipid.

It is important to realize that not all LNPs containing siRNA form these electron-dense particles per se. The formation of these electron-dense LNPs was shown to be dependent on the lipid formulation.<sup>[56]</sup> It was observed that an increase in DSPC content in an LNP formulation from 10 to 30 mol% resulted in lamellar structures on the outer layer of the LNP. This might not be surprising, as DSPC has a high propensity to form bilayers.<sup>[54]</sup> In addition, when the saturation of the acyl chains of ionizable amino-lipids was increased (using the dioleoyl analog of DLin-KC2-DMA), more bilayer structures arose around the electron-dense core.<sup>[56]</sup> Interestingly, an increase of ionizable amino-lipid above 70 mol% in a formulation containing 1 mol% PEG-lipid led to a decrease of siRNA encapsulation efficiency from  $\approx 90\%$  to  $\approx 60\%$ . At high concentrations of PEG-lipid (i.e., 5 mol%), a concentration of 50 mol% ionizable amino-lipid already led to a decrease in encapsulation efficiency from  $\approx 90\%$  to  $\approx 80\%$ . The influence of PEG-lipid on encapsulation efficiency was partly explained by the fact that higher concentrations of PEG-lipid led to smaller particles accompanying

higher surface-to-volume ratios whereby the ionizable amino-lipid would be exposed at the particles surface leaving the siRNA un-encapsulated. In addition, Leung et al. reasoned that the formation of the inverted micellar structure was not only caused by interaction of the ionizable amino-lipid with siRNA molecules but was aided by cholesterol and DSPC.<sup>[56]</sup> At high concentrations of cationic lipid, the amount of cholesterol in the particles was significantly lowered. The packing constraints of this combination of ionizable amino-lipid, cholesterol, DSPC, and PEG-lipid interfered with proper siRNA encapsulation. This effect could be counteracted by substitution of the DSPC lipid by DOPE. Compared to DSPC, DOPE has a more conical shape resulting in improved packing of the lipids at a high concentration of ionizable amino-lipid.<sup>[56]</sup>

Together, these findings indicate that the interplay between formulation and packing properties of lipid and nucleic acids largely determines the morphology of LNPs formed by SHM and that the electron-dense morphology of these LNPs deviates from the traditional lamellar structure of liposomes.<sup>[56]</sup> In addition, encapsulation efficiencies are influenced by the packing properties of specific lipid combinations.

### 3.3.4. Comparison of New Rapid-Mixing Techniques

It is challenging to directly compare the rapid-mixing methods since particle formulations tested between different methods vary. However, some general differences can be pointed out (Table 3).

The speed and type of mixing vary between methods. Mixing in SHM is based on chaotic advection, while mixing in MHF is based on convective–diffusive mixing, and mixing

in a T-junction is characterized as turbulent. The FRR differs between these methods. Particles in SHM and T-junction mixing are produced at lower FRRs compared to MHF, leading to higher concentrations of LNPs in SHM and T-junction mixing, since the percentage of the organic phase is higher. Furthermore, total flow rates, and thus arguably productivity, also differ between methods.<sup>[21,30,104]</sup>

An important issue in clinical translation is the ability to scale up production. For MHF, the VFF allows scaling up by vertically expanding the microfluidic setup, thereby increasing the output of the system. Scale-up of LNPs using SHM can be achieved relatively easily by parallelization of microfluidic chips or transition to larger-scale systems. T-junction mixing and cross-flow injection systems operate at a larger scale and are based on the similar principle of ethanol dilution.

### 3.3.5. Drawbacks of Rapid-Mixing Techniques

A drawback of all the abovementioned rapid-mixing techniques is that they incorporate a large amount of organic solvent in the manufacturing process, which can be present in the final product and bear an explosion risk at manufacturing scales. Additionally, strict guidelines exist for the amount of residual solvent present in parenteral therapeutics. Ethanol is the preferred solvent, as it can easily be removed using dialysis, and concentrations up to 0.5% (v/v) are accepted under the current guidelines in Europe and America (Ph.Eur. and USP, respectively). Another disadvantage of rapid-mixing systems is the limited solubility of some lipids in ethanol resulting in lower concentrations of LNPs in the mixed solutions. Ultrafiltration (e.g., by tangential flow filtration) can be used to concentrate

**Table 3.** Comparison of different production methods for LNP–siRNA.

Production method	Advantages	Disadvantages
Lipid film hydration + extrusion	<ul style="list-style-type: none"> <li>- Easy to perform</li> <li>- Accessible</li> </ul>	<ul style="list-style-type: none"> <li>- Low encapsulation efficiency</li> <li>- Large-scale production might be challenging</li> <li>- Multistep production process, time consuming</li> <li>- Relies on the use of chloroform/methanol—tolerable residual solvent limits are much lower than ethanol (cannot perform with ethanol)</li> </ul>
Preformed vesicle method	<ul style="list-style-type: none"> <li>- Moderate encapsulation efficiency (70%)</li> <li>- Particle size</li> </ul>	<ul style="list-style-type: none"> <li>- Mixing is relatively uncontrolled</li> <li>- Requires high concentration of PEG-lipid which could decrease transfection efficiency</li> </ul>
Crossflow injection	<ul style="list-style-type: none"> <li>- Controlled mixing</li> <li>- Already in use for large-scale production</li> </ul>	<ul style="list-style-type: none"> <li>- Less suited for lab-scale production</li> <li>- No data present on LNP–siRNA</li> </ul>
SHM	<ul style="list-style-type: none"> <li>- Controlled mixing</li> <li>- High encapsulation efficiency (&gt;95%)</li> <li>- Uniform particles (PDI &lt; 0.1)</li> <li>- Easily scalable between small and large batches based on parallelization</li> <li>- Easy to implement and handle</li> </ul>	<ul style="list-style-type: none"> <li>- Limited use of solvents due to cyclic olefin copolymer</li> <li>- Clogging of micro channels might occur</li> <li>- Requires parallelization for scale-up</li> </ul>
MHF	<ul style="list-style-type: none"> <li>- Controlled mixing environment</li> <li>- High encapsulation efficiency (≈70%)</li> </ul>	<ul style="list-style-type: none"> <li>- Mixing is slower at low FRRs</li> <li>- High FRRs lead to low particle concentrations</li> <li>- Requires parallelization for scale-up</li> </ul>
T-junction	<ul style="list-style-type: none"> <li>- Controlled rapid mixing</li> <li>- High encapsulation efficiency</li> <li>- Uniform particles</li> <li>- Broad solvent compatibility</li> </ul>	<ul style="list-style-type: none"> <li>- Less suited for lab-scale production</li> <li>- Requires parallelization for scale-up</li> </ul>

the LNP suspension. Furthermore, mixing using SHM may create solvent incompatibilities as the mixers are produced with poly(dimethylsiloxane) or cyclic olefin copolymer.<sup>[132]</sup> It is reported that this is not the case for T-junction mixing.<sup>[117]</sup>

When it comes to ease of implementation and use of each of these techniques, SHM is available “off-the-shelf,” similar to microfluidic hydrodynamic focusing devices. Systems for T-junction mixing are not readily available, and a production platform has to be set up on a case-by-case basis.

#### 4. State-of-the-Art Production of Lipid Nanoparticles Encapsulating mRNA, pDNA, and CRISPR/Cas9 Components

LNPs have also been used for the encapsulation of other nucleic acids besides siRNAs, such as mRNA, pDNA, and CRISPR/Cas9 components.<sup>[17,133–144]</sup> The use of similar lipid materials for encapsulating nucleic acids other than siRNA may be challenging, as mRNA, pDNA, and sgRNA are larger molecules and contain more negative charges and will not per se result in nanoparticles with an electron-dense LNP morphology. Here, the development of nanoparticles encapsulating mRNA, pDNA, and sgRNA is discussed.

##### 4.1. Design of Experimental Approaches to Develop LNP–mRNA

It is evident that mRNA and siRNA structurally differ based on size and charge. These differences might result in variations of lipid packing and LNP structure.<sup>[133]</sup> Several approaches have been used to adapt LNPs for the delivery of mRNA: changing the ratios of different lipids in the formulation<sup>[17]</sup> as well as the development of new, proprietary lipids<sup>[133–136]</sup> and a combination of both.<sup>[138]</sup>

Formulation optimization for the delivery of such payloads has been largely based on one-factor-at-a-time (OFAT) studies.<sup>[17]</sup> In OFAT studies, only one factor (or variable) is changed, while the other variables remain constant. A general drawback of such studies is that a possible optimal formulation might be overlooked due to the fact that higher order (second and third) interactions between variables (e.g., lipids in the formulation) are ignored.<sup>[145]</sup> The implication for formulation design is that changing only one lipid in the formulation at a time ignores possible interactions between the lipid constituents of a LNP/liposome, which might lead to suboptimal formulations. Alternatively, more optimal formulations are potentially overlooked due to limited sampling or changes in variables that are too small. In contrast, a design-of-experiment (DoE) approach, which aims to maximize the gain of information using a minimal amount of experiments, leading to a more efficient use of resources.<sup>[17,145]</sup> A DoE approach for the formulation of microfluidic-manufactured LNPs containing EPO-mRNA and the lipid C12-200 resulted in an approximately sevenfold increase in efficacy over the formulation initially optimized for siRNA (C12-200/DSPC/cholesterol/C14-PEG; 50/10/38.5/1.5 mol%).<sup>[44]</sup> Compared to LNP optimized for hepatic delivery of siRNA, the total amount of cationic lipid was

decreased from 50% to 35%; the helper lipid DSPC was substituted with DOPE; the amount of helper lipid was increased from 10% to 16% and the C14-PEG from 1.5 to 2.5%, resulting in an approximately sevenfold increase in serum erythropoietin (EPO) concentration in vivo. Analysis of the results obtained by this DoE experiment revealed that the choice of phospholipid (i.e., DOPE or DSPC) was the most important parameter for in vivo production of EPO. LNPs containing the phospholipid DOPE were superior in the ability to induce EPO production compared to LNPs containing DSPC. A second important parameter of efficacy was the weight ratio of C12-200 to mRNA. Additionally, several significant second-order interactions were found, such as an interaction between the mol% of C12-200 and the weight ratio of C12-200 to mRNA. The particle characteristics also changed: size decreased from 152 to 102 nm (DLS, intensity weighted), the polydispersity index increased from 0.102 to 0.158, and the zeta potential increased from –25.4 to –5.0 mV.<sup>[17]</sup>

When tailoring these particles for cancer immunotherapy, a new DoE was used based on various cationic lipids, which were synthesized by combinatorial chemistry.<sup>[43–45]</sup> Ovalbumin mRNA was formulated in a wide variety of LNPs and these particles were tested for their ability to induce a CD8 T-cell response. Parameters that were found to influence the percentage of antigen-specific CD8 T cells included the type of cationic lipid and mol% of cationic lipid favoring cKK-E12 and 10 mol%, respectively. The DoE approach resulted in an optimal formulation, B-11, containing cKK-E12/DOPE/cholesterol/PEG-C14/sodium lauryl sulfate (10/15/40.5/2.5/16 mol%). This formulation showed the best ability to generate an antigen-specific CD8 T-cell response 7 d after administration. The particle had an average size of 152 nm (DLS, intensity weighted; PDI: 0.217) with a multilamellar morphology. Cell types, other than hepatocytes, such as neutrophils and dendritic cells, were also successfully transfected. A single immunization with particles containing mRNA encoding tumor-associated antigens gp100 and TLR2 led to a strong CD8<sup>+</sup> T-cell response leading to tumor shrinkage in mice.<sup>[137]</sup> These data illustrate the value of DoE over an OFAT design in developing more potent LNPs. Based on the therapeutic strategy for which the LNPs are employed, e.g., protein expression versus cancer immunology, distinct optimal formulations were found. The formulation of ovalbumin mRNA differed in physicochemical properties from the siRNA optimized formulation in terms of particle morphology and size/charge.

Various new proprietary ionizable lipids with novel functionalities have been developed to improve the efficacy of LNP–mRNA formulations. Vaccines containing a newly developed proprietary lipid from Acuitas Therapeutics were used in an LNP formulation containing an ionizable lipid/helper lipid/cholesterol/PEG lipid in a molar ratio of 50/10/38.5/1.5 mol% lipid as a vaccine against the Zika virus. Mice and nonhuman primates were protected against challenges with Zika virus 5 months or 5 weeks after administration of these LNPs, respectively.<sup>[139]</sup> Currently, an mRNA vaccine against H10N8 is being tested in a Phase-I clinical trial, for which the interim results indicate a sound prophylactic response accompanied by mild-to-moderate adverse effects.<sup>[135]</sup> Weissman and co-workers also showed that a formulation similar to the LNP

used for siRNA delivery was used to passively immunize mice against a challenge with HIV-1.<sup>[146]</sup> LNPs encapsulating mRNA encoding an anti-HIV-1 antibody were successfully delivered to the liver resulting in the production of a monoclonal antibody protecting mice from an HIV-1 challenge.<sup>[146]</sup> The ionizable lipid that was used in this formulation has not been reported in the public domain. Ramaswamy et al. used a proprietary ionizable amino-lipid from Arcturus Therapeutics (ATX) containing an ionizable amino head group and a biodegradable lipid tail containing a cleavable ester bonds for the hepatic delivery of human factor IX mRNA.<sup>[133]</sup> By incorporating ester bonds in the acyl chains, the lipid was made biodegradable. Incorporation of this feature could be beneficial in terms of biocompatibility. For such LNPs, some constituents were enzymatically degraded and eliminated upon delivery of their content.<sup>[147]</sup> When the proprietary lipid was compared to DLin-MC3-DMA for both the delivery of siRNA and mRNA using payload-optimized formulations in mice, it was found to lead to five times more efficient gene silencing and two times higher protein expression, respectively.<sup>[133]</sup> In a quest to develop new LLMs for improved in vivo delivery of mRNA, Li et al. evaluated lipid-like nanoparticles as an alternative to LNPs containing ionizable amino-lipids. Particles containing the lipid-like molecule O-TT3 were able to deliver mRNA encoding human factor IX to mice resulting in the expression of factor IX at therapeutic levels.<sup>[136]</sup>

Fenton et al. recently claimed to have developed the most potent lipid known for mRNA delivery, referred to as OF-02, outperforming both cKK-E12 and C12-200.<sup>[138]</sup> The development of these optimized lipids, ATX and OF-02, for the delivery of mRNA is likely a preface for more potent LNPs carrying nucleic acids in the future. It is interesting to note that LNPs containing the biodegradable variant of OF-02 resulted in an increased protein expression in the spleen compared to the liver. However, particle tracking showed that most particles accumulated in the liver while only 15% of the expressed protein originated there. When the nondegradable OF-02 lipid was used, protein expression was not observed in the spleen, rather only in the liver. These observations are still not fully explained; however, they indicate that, based on lipid composition, particles might be directed to either liver protein expression or spleen protein expression.<sup>[140]</sup>

#### 4.2. LNPs for the Delivery of pDNA

LNPs can be utilized as a transfection reagent to introduce pDNA to eukaryotic cells in order to induce sustained protein expression. Only a limited amount of data is available on the adaption of LNPs for the formulation of pDNA. It has to be mentioned that the use of LNP-pDNA is limited to dividing cells, since these particles do not facilitate nuclear entry and therefore pDNA access to the nucleus is restricted to conditions wherein the nuclear membrane is temporarily compromised (as in cell division).<sup>[148–150]</sup> Several ionizable amino-lipids, namely DLin-MC3-DMA, DLin-KC2-DMA, and DLin-DMA, have been evaluated for their use for the delivery of pDNA. Superior results were obtained using the lipid DLin-KC2-DMA over DLin-MC3-DMA.<sup>[32]</sup> Moreover, the influence of the helper lipid within the formulation containing DLin-KC2-DMA was tested. When the helper lipid DSPC was substituted with unsaturated phosphatidylcholines

(1-stearoyl-2-oleoyl-sn-glycero-3-phosphocholine (SOPC) or DOPC) additional improvement of the particles' transfection efficacy was obtained.<sup>[32]</sup> In these formulations, the helper lipid had no influence on the particle electron-dense core morphology. Interestingly, when HeLa cultures were treated with LNPs in a medium containing fetal bovine serum (FBS), DOPC, and SOPC showed significant improvements over DSPC-LNPs. When the FBS was replaced with murine serum, DOPE formulations showed significant improvements. This suggests a clear role of serum components in modulating the efficacy of LNP formulations. Furthermore, PEG-lipids were observed to influence the transfection efficacy of lipoplexes encapsulating pDNA. Transfection efficacy was shown to be dependent on the acyl chain length of the PEG-lipid favoring shorter acyl chains since they diffuse more rapidly from the liposomal membrane exposing the cationic surface needed for efficient DNA transfections.<sup>[51]</sup>

#### 4.3. LNPs for the Functional Delivery of Components of the CRISPR-Cas9 Genome-Editing System

CRISPR is a prokaryotic adaptive immune system<sup>[151]</sup> that has been successfully modified for human-gene-editing purposes.<sup>[152,153]</sup> One of the CRISPR systems used for mammalian genome editing is composed of the Cas9 enzyme (e.g., *Streptococcus pyogenes* Cas9) accompanied by an sgRNA.<sup>[152]</sup> The sgRNA molecules mediate sequence-specific cleavage of DNA by the Cas9 enzyme, resulting in a double-strand break (DSB) of the targeted DNA.<sup>[152]</sup> The subsequent activation of the endogenous repair mechanism of nonhomologous end joining may lead to permanent suppression of a target gene. In contrast, by activation of homology-directed repair, a specific gene sequence can be inserted, if a DNA template with sequence homology to the flanking nucleotides of the DSB site is present.<sup>[154]</sup>

The components of the CRISPR-Cas9 system can be delivered in various forms, such as mRNA, pDNA, or as an sgRNA-protein complex.<sup>[10]</sup> The delivery of sgRNA/mRNA/pDNA is hampered by similar issues as siRNA.<sup>[155]</sup> Therefore, delivery systems are a prerequisite for in vivo applications of CRISPR/Cas9, and LNPs might provide a valuable option for this purpose.<sup>[156]</sup> LNP-mediated Cas9 mRNA delivery is especially challenging considering the Cas9 mRNA length of  $\approx 4500$  nt.<sup>[141]</sup>

Both existing and novel lipids/LLMs have been proposed for delivery of CRISPR/Cas9 elements in vivo. For example, C12-200 was used to formulate Cas9-mRNA in LNPs. Co-administration of LNP-Cas9 mRNA with an adeno-associated viral particle encoding an sgRNA and a DNA donor template led to correction of mice hepatocytes containing a mutated gene coding for fumarylacetate hydrolase. Systemic administration led to a correction of  $6.2 \pm 1.0\%$  of the hepatocytes as observed by immuno-histochemistry.<sup>[142]</sup> In addition, several novel lipids/LLMs have been developed concurrently with the specific aim of delivering sgRNA and Cas9 (as protein or mRNA). Examples include 3-014B, MPA-A&AB, and ZA3-EP10.<sup>[141,143,144]</sup> Nanoparticles containing the biodegradable lipid 3-014B were able to form nanoparticles with Cas9/sgRNA-complexes.<sup>[143]</sup> The resulting structures were relatively large ( $\approx 292 \pm 15.3$  nm) and slightly negatively charged. When HEK293T cells expressing enhanced green fluorescent protein (eGFP) were incubated

with these LNPs at concentrations of  $25 \times 10^{-9}$  M of Cas9:sgRNA with  $6 \mu\text{g mL}^{-1}$  lipid, a 70% reduction in eGFP expression was observed.<sup>[143]</sup> However, the feasibility of these particles for systemic administration (e.g., intravenous injection) can be questioned due to their unfavorable physicochemical properties.

In an attempt to improve the delivery of Cas9 mRNA, Zhang et al. developed several new biodegradable LLMs.<sup>[144]</sup> These LLMs were formulated in particles containing LLM/DOPE/cholesterol/DMG-PEG ( $\approx 22/33.1/44.1/0.8$  mol%). Both in vitro and in vivo data showed delivery of Cas9 mRNA to target cells. After incubation of cells stably expressing eGFP and eGFP sgRNA with nanoparticles at a dose of 50 ng Cas9 mRNA per well in a 24-well plate, a decrease in fluorescence intensity was observed. Furthermore, when these particles were administered intratumorally to mice carrying xenograft tumors of the earlier-mentioned eGFP-HEK293T cells, a decrease of 41% in eGFP fluorescence intensity was observed, indicating in vivo delivery of Cas9 mRNA to HEK293T tumors.<sup>[144]</sup> However, this murine model does not fully represent the challenge of delivering a complete CRISPR/Cas9 system in vivo as the model HEK293T cells already expressed eGFP sgRNA, which, in a drug product for commercial applications, needs to be co-delivered to the same cell.

Miller et al. developed zwitterionic amino lipids (ZALs) especially for the delivery of Cas9 mRNAs and sgRNAs.<sup>[141]</sup> These lipids incorporated, according to the authors, multiple characteristics derived from successful cationic and ionizable amino-lipids, as well as from zwitterionic lipids into a single lipid, which might improve the delivery of larger RNAs. ZAL ZA3-EP10 was efficient in delivering an sgRNA and an mRNA in vitro. Furthermore, these nanoparticles of unknown morphology containing ZA3-EP10, formulated with cholesterol and a PEG-lipid (ZAL/cholesterol/PEG-lipid; 56.18/43.26/0.56 mol%), produced using SHM, were able to deliver mRNA sequences for mCherry and luciferase. It was reasoned that co-delivery of sgRNA and mRNA encapsulated within a single nanoparticle is beneficial since both are needed for efficient genome editing.<sup>[141]</sup> Therefore, they co-formulated mRNA and sgRNA in a ratio of 3:1 (w/w) and reported successful co-delivery of Cas9 mRNA and an sgRNA in vivo. Mice expressing the Rosa26 promoter Lox-Stop-Lox tdTomato (tdTO) cassette were injected with a particle containing an sgRNA targeting the LoxP sequence. In this reporter setup, successful delivery of mRNA and sgRNA would lead to deletion of the stop-sequence enabling expression of the tdTO resulting in a fluorescence signal. Intravenous administration of the particles resulted in a fluorescence signal within the lungs, kidney, and liver.<sup>[141]</sup> Interestingly, several companies involved in CRISPR/Cas9 gene editing are exploring the possibilities of LNP-mediated gene delivery, indicating that LNPs are considered as a suitable option for the delivery of the CRISPR/Cas9 system.<sup>[157,158]</sup>

As discussed above, different approaches have been used to optimize LNPs for the delivery of mRNA/pDNA/sgRNA using microfluidic manufacturing. Both optimization of the lipid formulation and the development of new proprietary lipids have resulted in significant improvements and impressive pre-clinical results for in vivo models. Data of LNPs containing different nucleic acid payloads indicate that initial optimized formulations for siRNA delivery cannot be extrapolated to mRNA, pDNA, or sgRNA carrying nanoparticles, but need to

be adapted to their specific nucleic acid cargo. The use of a DoE approach has resulted in significant improvements of several formulations, illustrating its added value in optimizing lipid formulations for in vivo efficacy. In the future, DoE approaches may be of substantial importance when tailoring nucleic-acid-loaded particles to other cells than cell types described here.

## 5. Future Perspectives/Conclusions

The use of LNPs for RNA delivery has made tremendous progress over the past decade. In this light, the recent successful outcome of the Phase-III study on Patisiran may, for the time being, be considered a highpoint for the field.

A key development has been the design of ionizable amino-lipids that are neutral at physiological pH as a replacement for permanently charged cationic lipids. This avoids nonspecific interactions with blood components and nontarget cells. In addition, small structural variations in these ionizable amino-lipids have been shown to result in large improvements in functional delivery. These improvements are not always well understood. The continuing emergence of novel lipids with high efficiency may help in identifying and rationally optimizing ionizable amino-lipid component of LNPs even further.

The development of sheddable PEG-coatings represents a balancing act between particle stability during production in the circulation on the one hand, and subsequent regulated opsonization with desired proteins, such as ApoE, and triggered exposure of an interactive surface, on the other. The gradual loss of PEG from the LNP through the use of short-chain ceramides helps to make these seemingly incompatible demands meet.

Up to now, opsonization by ApoE in vivo has enabled hepatocyte delivery, but delivery to other tissues remains challenging. Modulation of the particle surface to attract other opsonins may help to reach other tissues beyond the liver.

The initial observational studies on LNP performance has yielded a broad set of design characteristics for LNP-siRNA. However, it has to be kept in mind that some of these physicochemical properties are only general guidelines.<sup>[159]</sup> Further insight into the relationship between a nanoparticle's physicochemical properties and its efficacy might lead to further improvements of LNPs potency. An important step to establish the best characteristics may be increased use of DoE-based optimization. Using DoE analysis, higher-order relationships between LNP composition, characteristics, and performance may be uncovered. A prerequisite for clinical development is the reproducible and scalable manufacturing of tunable LNPs. The development of rapid-mixing methods, described here, provides a platform for the production of such systems. The use of rapid-mixing methods is currently being applied to other nucleic acids, such as mRNA and sgRNA. The development of LNPs encapsulating these RNA types has made clear that formulations need to be optimized for each type of nucleic acid payload and are certainly not interchangeable. Early success has been shown for LNPs encapsulating mRNA with applications in single-dose vaccines for Zika virus, influenza virus H10N8 and H7N9, as well as protein replacement therapy for FIX IX and EPO.<sup>[17,133–135,139]</sup> These developments further highlight that LNPs are a versatile platform for unlocking the therapeutic potential of several types of nucleic-acid-based therapeutics.

## Acknowledgements

The work of M.J.W.E. and R.M.S. on LNPs had received funding from the European Union's Horizon 2020 research and innovation programme under grant agreement No. 721058. R.v.d.M. (# 14385) and P.V. (# 13667) were supported by a VENI Fellowship from the Netherlands Organization for Scientific Research (NWO). The work undertaken by J.A.K. and P.R.C. was funded by a Foundation Grant from the Canadian Institute for Health Research (FDN 148469).

## Conflict of Interest

The authors declare no conflict of interest.

## Keywords

gene editing, lipid nanoparticles, microfluidics, production methods, siRNA delivery

Received: November 20, 2017

Revised: January 20, 2018

Published online: April 26, 2018

- [1] A. Wittrup, J. Lieberman, *Nat. Rev. Genet.* **2015**, *16*, 543.
- [2] P. R. Cullis, M. J. Hope, *Mol. Ther.* **2017**, *25*, 1467.
- [3] Alnylam Pharmaceuticals Inc., Alnylam and Sanofi Report Positive Topline Results from APOLLO Phase 3 Study of Patisiran in Hereditary ATTR (hATTR) Amyloidosis Patients with Polyneuropathy, <http://investors.alnylam.com/releasedetail.cfm?ReleaseID=1041081> (accessed: October 2017).
- [4] Alnylam Pharmaceuticals Inc., Alnylam Completes Submission of New Drug Application to U.S. Food and Drug Administration (FDA) for Patisiran for the Treatment of Hereditary ATTR (hATTR) Amyloidosis, <http://investors.alnylam.com/news-releases/news-release-details/alnylam-completes-submission-new-drug-application-us-food-and> (accessed: January 2018).
- [5] K. A. Whitehead, R. Langer, D. G. Anderson, *Nat. Rev. Drug Discovery* **2009**, *8*, 129.
- [6] Y. Y. C. Tam, S. Chen, P. R. Cullis, *Pharmaceutics* **2013**, *5*, 498.
- [7] A. Fire, S. Xu, M. K. Montgomery, S. A. Kostas, S. E. Driver, C. C. Mello, *Nature* **1998**, *391*, 806.
- [8] C. Matranga, Y. Tomari, C. Shin, D. P. Bartel, P. D. Zamore, *Cell* **2005**, *123*, 607.
- [9] S. L. Ameres, J. Martinez, R. Schroeder, *Cell* **2007**, *130*, 101.
- [10] J. C. Kaczmarek, P. S. Kowalski, D. G. Anderson, *Genome Med.* **2017**, *9*, 60.
- [11] J. A. Wolff, R. W. Malone, P. Williams, W. Chong, G. Acsadi, A. Jani, P. L. Felgner, *Science* **1990**, *247*, 1465.
- [12] J. A. Doudna, E. Charpentier, *Science* **2014**, *346*, 1258096-1.
- [13] H. Yin, R. L. Kanasty, A. A. Eltoukhy, A. J. Vegas, J. R. Dorkin, D. G. Anderson, *Nat. Rev. Genet.* **2014**, *15*, 541.
- [14] R. Kanasty, J. R. Dorkin, A. Vegas, D. Anderson, *Nat. Mater.* **2013**, *12*, 967.
- [15] R. L. Juliano, *Nucleic Acids Res.* **2016**, *44*, 6518.
- [16] X. Shen, D. R. Corey, *Nucleic Acids Res.* **2017**, *46*, 1584.
- [17] K. J. Kauffman, J. R. Dorkin, J. H. Yang, M. W. Heartlein, F. Derosa, F. F. Mir, O. S. Fenton, D. G. Anderson, *Nano Lett.* **2015**, *15*, 7300-6.
- [18] S. C. Semple, A. Akinc, J. Chen, A. P. Sandhu, B. L. Mui, C. K. Cho, D. W. Y. Sah, D. Stebbing, E. J. Crosley, E. Yaworski, I. M. Hafez, J. R. Dorkin, J. Qin, K. Lam, K. G. Rajeev, K. F. Wong, L. B. Jeffs, L. Nechev, M. L. Eisenhardt, M. Jayaraman, M. Kazem, M. A. Maier, M. Srinivasulu, M. J. Weinstein, Q. Chen, R. Alvarez, S. A. Barros, S. De, S. K. Klimuk, T. Borland, V. Kosovrasti, W. L. Cantley, Y. K. Tam, M. Manoharan, M. A. Ciufolini, M. A. Tracy, A. de Fougères, I. MacLachlan, P. R. Cullis, T. D. Madden, M. J. Hope, *Nat. Biotechnol.* **2010**, *28*, 172.
- [19] M. Jayaraman, S. M. Ansell, B. L. Mui, Y. K. Tam, J. Chen, X. Du, D. Butler, L. Eltepu, S. Matsuda, J. K. Narayanannair, K. G. Rajeev, I. M. Hafez, A. Akinc, M. A. Maier, M. A. Tracy, P. R. Cullis, T. D. Madden, M. Manoharan, M. J. Hope, *Angew. Chem., Int. Ed.* **2012**, *51*, 8529.
- [20] I. V. Zhigaltsev, N. Belliveau, I. Hafez, A. K. K. Leung, J. Huft, C. Hansen, P. R. Cullis, *Langmuir* **2012**, *28*, 3633.
- [21] N. M. Belliveau, J. Huft, P. J. Lin, S. Chen, A. K. Leung, T. J. Leaver, A. W. Wild, J. B. Lee, R. J. Taylor, Y. K. Tam, C. L. Hansen, P. R. Cullis, *Mol. Ther.–Nucleic Acids* **2012**, *1*, e37.
- [22] D. W. Deamer, *FASEB J.* **2010**, *24*, 1308.
- [23] G. Gregoriadis, *FEBS Lett.* **1973**, *36*, 292.
- [24] G. J. Dimitriadis, *FEBS Lett.* **1978**, *86*, 289.
- [25] G. Gregoriadis, P. D. Leathwood, B. E. Ryman, *FEBS Lett.* **1971**, *14*, 95.
- [26] G. Gregoriadis, *Pharmaceutics* **2016**, *8*, 1.
- [27] V. P. Torchilin, *Nat. Rev. Drug Discovery* **2005**, *4*, 145.
- [28] S. C. Semple, S. K. Klimuk, T. O. Harasym, N. Dos Santos, S. M. Ansell, K. F. Wong, N. Maurer, H. Stark, P. R. Cullis, M. J. Hope, P. Scherrer, *Biochim. Biophys. Acta* **2001**, *1510*, 152.
- [29] K. Buyens, J. Demeester, S. S. De Smedt, N. N. Sanders, *Langmuir* **2009**, *25*, 4886.
- [30] M. T. Abrams, M. L. Koser, J. Seitzer, S. C. Williams, M. A. DiPietro, W. Wang, A. W. Shaw, X. Mao, V. Jadhav, J. P. Davide, P. A. Burke, A. B. Sachs, S. M. Stirdivant, L. Sepp-Lorenzino, *Mol. Ther.* **2010**, *18*, 171.
- [31] L. B. Jeffs, L. R. Palmer, E. G. Ambegia, C. Giesbrecht, S. Ewanick, I. MacLachlan, *Pharm. Res.* **2005**, *22*, 362.
- [32] J. A. Kulkarni, J. L. Myhre, S. Chen, Y. C. Y. Tam, A. Danescu, J. M. Richman, P. R. Cullis, *Nanomedicine* **2016**, *13*, 1377.
- [33] A. K. K. Leung, I. M. Hafez, S. Baoukina, N. M. Belliveau, I. V. Zhigaltsev, E. Afshinmanesh, D. P. Tieleman, C. L. Hansen, M. J. Hope, P. R. Cullis, *J. Phys. Chem. C* **2012**, *116*, 18440.
- [34] R. Krzysztóń, B. Salem, D. J. Lee, G. Schwake, E. Wagner, J. O. Rädler, *Nanoscale* **2017**, *9*, 7442.
- [35] R. Crawford, B. Dogdas, E. Keough, R. M. Haas, W. Wepukhulu, S. Krotzer, P. Burke, L. Sepp-Lorenzino, A. Bagchi, B. J. Howell, *Int. J. Pharm.* **2011**, *403*, 237.
- [36] R. A. Petros, J. M. DeSimone, *Nat. Rev. Drug Discovery* **2010**, *9*, 615.
- [37] E. Blanco, H. Shen, M. Ferrari, *Nat. Biotechnol.* **2015**, *33*, 941.
- [38] A. Chonn, S. C. Semple, P. R. Cullis, *J. Biol. Chem.* **1992**, *267*, 18759.
- [39] I. M. Hafez, N. Maurer, P. R. Cullis, *Gene Ther.* **2001**, *8*, 1188.
- [40] Y. Xu, F. C. Szoka, *Biochemistry* **1996**, *35*, 5616.
- [41] J. A. Heyes, L. Palmer, K. Bremner, I. MacLachlan, *J. Controlled Release* **2005**, *107*, 276.
- [42] A. Akinc, A. Zumbuehl, M. Goldberg, E. S. Leshchiner, V. Busini, N. Hossain, S. A. Bacallado, D. N. Nguyen, J. Fuller, R. Alvarez, A. Borodovsky, T. Borland, R. Constien, A. de Fougères, J. R. Dorkin, K. Narayanannair Jayaprakash, M. Jayaraman, M. John, V. Koteliansky, M. Manoharan, L. Nechev, J. Qin, T. Racie, D. Raitcheva, K. G. Rajeev, D. W. Y. Sah, J. Soutschek, I. Toudjarska, H.-P. Vornlocher, T. S. Zimmermann, R. Langer, D. G. Anderson, *Nat. Biotechnol.* **2008**, *26*, 561.
- [43] Y. Dong, K. T. Love, J. R. Dorkin, S. Sirirungruang, Y. Zhang, D. Chen, R. L. Bogorad, H. Yin, Y. Chen, A. J. Vegas, C. a. Alabi, G. Sahay, K. T. Olejnik, W. Wang, A. Schroeder, A. K. R. Lytton-Jean, D. J. Siegwart, A. Akinc, C. Barnes, S. A. Barros, M. Carioto,

- K. Fitzgerald, J. Hettinger, V. Kumar, T. I. Novobrantseva, J. Qin, W. Querbes, V. Koteliensky, R. Langer, D. G. Anderson, *Proc. Natl. Acad. Sci. USA* **2014**, *111*, 3955.
- [44] K. T. Love, K. P. Mahon, C. G. Levins, K. A. Whitehead, W. Querbes, J. R. Dorkin, J. Qin, W. Cantley, L. L. Qin, T. Racie, M. Frank-Kamenetsky, K. N. Yip, R. Alvarez, D. W. Y. Sah, A. de Fougères, K. Fitzgerald, V. Koteliensky, A. Akinc, R. Langer, D. G. Anderson, *Proc. Natl. Acad. Sci. USA* **2010**, *107*, 1864.
- [45] K. A. Whitehead, J. R. Dorkin, A. J. Vegas, P. H. Chang, J. Matthews, O. S. Fenton, Y. Zhang, K. T. Olejnik, V. Yesilyurt, D. Chen, S. Barros, B. Klebanov, T. Novobrantseva, R. Langer, D. G. Anderson, *Nat. Commun.* **2014**, *5*, 4277.
- [46] N. Yamamoto, Y. Sato, T. Munakata, M. Kakuni, C. Tateno, T. Sanada, Y. Hirata, S. Murakami, Y. Tanaka, K. Chayama, H. Hatakeyama, M. Hyodo, H. Harashima, M. Kohara, *J. Hepatol.* **2016**, *64*, 547.
- [47] Y. Sato, H. Hatakeyama, Y. Sakurai, M. Hyodo, H. Akita, H. Harashima, *J. Controlled Release* **2012**, *163*, 267.
- [48] I. M. Hafez, P. R. Cullis, *Adv. Drug Delivery Rev.* **2001**, *47*, 139.
- [49] P. R. Cullis, B. De Kruijff, *Biochim. Biophys. Acta, Biomembr.* **1978**, *513*, 31.
- [50] H. Farhood, N. Serbina, L. Huang, *Biochim. Biophys. Acta, Biomembr.* **1995**, *1235*, 289.
- [51] K. W. C. Mok, A. M. I. Lam, P. R. Cullis, *Biochim. Biophys. Acta, Biomembr.* **1999**, *1419*, 137.
- [52] M. J. Hope, B. Mui, S. Ansell, Q. F. Ahkong, *Mol. Membr. Biol.* **1998**, *15*, 1.
- [53] X. Cheng, R. J. Lee, *Adv. Drug Delivery Rev.* **2016**, *99*, 129.
- [54] J. L. Thewalt, M. Bloom, *Biophys. J.* **1992**, *63*, 1176.
- [55] A. K. K. Leung, *Ph.D. Thesis*, The University of British Columbia (Vancouver, Canada) **2015**.
- [56] A. K. K. Leung, Y. Y. C. Tam, S. Chen, I. M. Hafez, P. R. Cullis, *J. Phys. Chem. B* **2015**, *119*, 8698.
- [57] R. A. Demel, B. De Kruijff, *Biochim. Biophys. Acta* **1976**, *457*, 109.
- [58] W.-C. Hung, M.-T. Lee, F.-Y. Chen, H. W. Huang, *Biophys. J.* **2007**, *92*, 3960.
- [59] R. A. Demel, K. R. Bruckdorfer, L. L. M. Van Deenen, *Biochim. Biophys. Acta, Biomembr.* **1972**, *255*, 321.
- [60] D. Papahadjopoulos, S. Nir, S. Ohki, *Biochim. Biophys. Acta* **1971**, *266*, 561.
- [61] S. C. Semple, A. Chonn, P. R. Cullis, *Biochemistry* **1996**, *35*, 2521.
- [62] W. V. Rodriguez, P. Haydn Pritchard, M. J. Hope, *Biochim. Biophys. Acta, Biomembr.* **1993**, *1153*, 9.
- [63] W. V. Rodriguez, S. K. Klimuk, C. N. Kitson, J. J. Wheeler, M. J. Hope, *Biochemistry* **1995**, *34*, 6208.
- [64] C. Kirby, J. Clarke, G. Gregoriadis, *FEBS Lett.* **1980**, *111*, 324.
- [65] T. M. Allen, *Adv. Drug Delivery Rev.* **1994**, *13*, 285.
- [66] S. Chen, Y. Y. C. Tam, P. J. C. Lin, M. M. H. Sung, Y. K. Tam, P. R. Cullis, *J. Controlled Release* **2016**, *235*, 236.
- [67] Y. Bao, Y. Jin, P. Chivukula, J. Zhang, Y. Liu, J. Liu, J.-P. Clamme, R. I. Mahato, D. Ng, W. Ying, Y. Wang, L. Yu, *Pharm. Res.* **2013**, *30*, 342.
- [68] S. Chen, Y. Y. C. Tam, P. J. C. Lin, A. K. K. Leung, Y. K. Tam, P. R. Cullis, *J. Controlled Release* **2014**, *196*, 106.
- [69] B. L. Mui, Y. K. Tam, M. Jayaraman, S. M. Ansell, X. Du, Y. Y. C. Tam, P. J. Lin, S. Chen, J. K. Narayanannair, K. G. Rajeev, M. Manoharan, A. Akinc, M. A. Maier, P. Cullis, T. D. Madden, M. J. Hope, *Mol. Ther.–Nucleic Acids* **2013**, *2*, e139.
- [70] A. Akinc, W. Querbes, S. De, J. Qin, M. Frank-Kamenetsky, K. N. Jayaprakash, M. Jayaraman, K. G. Rajeev, W. L. Cantley, J. R. Dorkin, J. S. Butler, L. Qin, T. Racie, A. Sprague, E. Fava, A. Zeigerer, M. J. Hope, M. Zerial, D. W. Y. Sah, K. Fitzgerald, M. A. Tracy, M. Manoharan, V. Koteliensky, A. de Fougères, M. A. Maier, *Mol. Ther.* **2010**, *18*, 1357.
- [71] S. Mishra, P. Webster, M. E. Davis, *Eur. J. Cell Biol.* **2004**, *83*, 97.
- [72] H. Hatakeyama, H. Akita, K. Kogure, M. Oishi, Y. Nagasaki, Y. Kihira, M. Ueno, H. Kobayashi, H. Kikuchi, H. Harashima, *Gene Ther.* **2007**, *14*, 68.
- [73] M. S. Webb, D. Saxon, F. M. P. Wong, H. J. Lim, Z. Wang, M. B. Bally, L. S. L. Choi, P. R. Cullis, L. D. Mayer, *Biochim. Biophys. Acta, Biomembr.* **1998**, *1372*, 272.
- [74] E. Ambegia, S. Ansell, P. Cullis, J. Heyes, L. Palmer, I. MacLachlan, *Biochim. Biophys. Acta* **2005**, *1669*, 155.
- [75] S. C. Semple, T. O. Harasym, K. A. Clow, S. M. Ansell, S. K. Klimuk, M. J. Hope, *J. Pharmacol. Exp. Ther.* **2005**, *312*, 1020.
- [76] J. B. Lee, K. Zhang, Y. Y. C. Tam, J. Quick, Y. K. Tam, P. J. Lin, S. Chen, Y. Liu, J. K. Nair, I. Zlatev, K. G. Rajeev, M. Manoharan, P. S. Rennie, P. R. Cullis, *Mol. Ther.–Nucleic Acids* **2016**, *5*, e348, <https://doi.org/10.1038/mtna.2016.43>.
- [77] H. Harashima, H. Kiwada, *Adv. Drug Delivery Rev.* **1996**, *19*, 425.
- [78] E. Wisse, F. Jacobs, B. Topal, P. Frederik, B. De Geest, *Gene Ther.* **2008**, *15*, 1193.
- [79] A. U. Andar, R. R. Hood, W. N. Vreeland, D. L. Devoe, P. W. Swaan, *Pharm. Res.* **2014**, *31*, 401.
- [80] T. Kirchhausen, *Trends Cell Biol.* **2009**, *19*, 596.
- [81] B. Yameen, W. Il Choi, C. Vilos, A. Swami, J. Shi, O. C. Farokhzad, *J. Controlled Release* **2014**, *190*, 485.
- [82] G. Sahay, W. Querbes, C. Alabi, A. Eltoukhy, S. Sarkar, C. Zurenko, E. Karagiannis, K. Love, D. Chen, R. Zoncu, Y. Buganim, A. Schroeder, R. Langer, D. G. Anderson, *Nat. Biotechnol.* **2013**, *31*, 653.
- [83] J. Gilleron, W. Querbes, A. Zeigerer, A. Borodovsky, G. Marsico, U. Schubert, K. Manygoats, S. Seifert, C. Andree, M. Stoter, H. Epstein-Barash, L. Zhang, V. Koteliensky, K. Fitzgerald, E. Fava, M. Bickle, Y. Kalaidzidis, A. Akinc, M. Maier, M. Zerial, *Nat. Biotechnol.* **2013**, *31*, 638.
- [84] A. Wittrup, A. Ai, X. Liu, P. Hamar, R. Trifonova, K. Charisse, M. Manoharan, T. Kirchhausen, J. Lieberman, *Nat. Biotechnol.* **2015**, *33*, 870.
- [85] L. A. Meure, N. R. Foster, F. Dehghani, *AAPS PharmSciTech* **2008**, *9*, 798.
- [86] N. Grimaldi, F. Andrade, N. Segovia, L. Ferrer-Tasies, S. Sala, J. Veciana, N. Ventosa, *Chem. Soc. Rev.* **2016**, *45*, 6520.
- [87] E. Elizondo, E. Moreno, I. Cabrera, A. Córdoba, S. Sala, J. Veciana, N. Ventosa, *Prog. Mol. Biol. Transl. Sci.* **2011**, *104*, 1.
- [88] J. Lasch, V. Weissig, M. Brandl, in *Liposomes: A Practical Approach*, Vol. 2 (Eds: V. P. Torchilin, V. Weissig), Oxford University Press, Oxford, UK **2003**, Ch. 1.
- [89] F. Szoka, D. Papahadjopoulos, *Annu. Rev. Biophys. Bioeng.* **1980**, *9*, 467.
- [90] L. D. Mayer, M. J. Hope, P. R. Cullis, *Biochim. Biophys. Acta* **1986**, *858*, 161.
- [91] M. R. Mozafari, in *Liposomes, Method in Molecular Biology (Methods and Protocols)*, Vol. 1 (Ed: V. Weissig), Humana Press, New York, NY, USA **2010**, Ch. 2.
- [92] F. Szoka, D. Papahadjopoulos, *Proc. Natl. Acad. Sci. USA* **1978**, *75*, 4194.
- [93] E. Mayhew, R. Lazo, W. J. Vail, J. King, A. M. Green, *Biochim. Biophys. Acta, Biomembr.* **1984**, *775*, 169.
- [94] S. I. Kim, D. Shin, T. H. Choi, J. C. Lee, G.-J. Cheon, K.-Y. Kim, M. Park, M. Kim, *Mol. Ther.* **2007**, *15*, 1145.
- [95] K. Buyens, S. C. De Smedt, K. Braeckmans, J. Demeester, L. Peeters, L. a. Van Grunsven, X. De Mollerat Du Jeu, R. Sawant, V. Torchilin, K. Farkasova, M. Ogris, N. N. Sanders, *J. Controlled Release* **2012**, *158*, 362.
- [96] S. Batzri, E. D. Korn, *Biochim. Biophys. Acta, Biomembr.* **1973**, *298*, 1015.
- [97] A. Wagner, K. Vorauer-Uhl, G. Kreismayr, H. Katinger, *J. Liposome Res.* **2002**, *12*, 259.
- [98] A. Wagner, K. Vorauer-Uhl, *J. Drug Delivery* **2011**, *2011*, 1.

- [99] R. R. Hood, D. L. DeVoe, *Small* **2015**, *11*, 5790.
- [100] S. Garg, G. Heuck, S. Ip, E. Ramsay, *J. Drug Targeting* **2016**, *24*, 821.
- [101] C. Wan, T. M. Allen, P. R. Cullis, *Drug Delivery Transl. Res.* **2014**, *4*, 74.
- [102] R. Paliwal, R. J. Babu, S. Palakurthi, *AAPS PharmSciTech* **2014**, *15*, 1527.
- [103] N. Desai, *AAPS J.* **2012**, *14*, 282.
- [104] A. Jahn, W. N. Vreeland, M. Gaitan, L. E. Locascio, *J. Am. Chem. Soc.* **2004**, *126*, 2674.
- [105] C. Walsh, K. Ou, N. M. Belliveau, T. J. Leaver, A. W. Wild, J. Huft, P. J. Lin, S. Chen, A. K. Leung, J. B. Lee, C. L. Hansen, R. J. Taylor, E. C. Ramsay, P. R. Cullis, in *Drug Delivery Systems* (Ed: K. K. Jain), Springer, New York, NY **2014**, p. 109.
- [106] M. Hope, R. Nayar, L. Mayer, in *Liposome Technology* (Ed: G. Gregoriadis), CRC Press, Boca Raton, FL **1993**, p. 123.
- [107] H. O. Hauser, *Biochem. Biophys. Res. Commun.* **1971**, *45*, 1049.
- [108] B. S. Pattani, V. V. Chupin, V. P. Torchilin, *Chem. Rev.* **2015**, *115*, 10938.
- [109] A. Cern, D. Marcus, A. Tropsha, Y. Barenholz, A. Goldblum, *J. Controlled Release* **2017**, *252*, 18.
- [110] R. Koynova, B. Tenchov, *Recent Pat. Nanotechnol.* **2015**, *9*, 86.
- [111] Y. P. Patil, S. Jadhav, *Chem. Phys. Lipids* **2014**, *177*, 8.
- [112] P. M. Valencia, O. C. Farokhzad, R. Karnik, R. Langer, *Nat. Nanotechnol.* **2012**, *7*, 623.
- [113] C. Y. Lee, C. L. Chang, Y. N. Wang, L. M. Fu, *Int. J. Mol. Sci.* **2011**, *12*, 3263.
- [114] D. Carugo, E. Bottaro, J. Owen, E. Stride, C. Nastruzzi, *Sci. Rep.* **2016**, *6*, 25876.
- [115] S. Hirota, C. T. De Ilarduya, L. G. Barron, F. C. Szoka, *BioTechniques* **1999**, *27*, 286.
- [116] L. A. Davies, G. A. Nunez-Alonso, H. L. Hebel, R. K. Scheule, S. H. Cheng, S. C. Hyde, D. R. Gill, *BioTechniques* **2010**, *49*, 666.
- [117] J. A. Kulkarni, Y. Y. C. Tam, S. Chen, J. Zaifman, Y. K. Tam, P. R. Cullis, S. Biswas, *Nanoscale* **2017**, *9*, 13600.
- [118] T. S. Zimmermann, A. C. H. Lee, A. Akinc, B. Bramlage, D. Bumcrot, M. N. Fedoruk, J. Harborth, J. A. Heyes, L. B. Jeffs, M. John, A. D. Judge, K. Lam, K. McClintock, L. V. Nechev, L. R. Palmer, T. Racie, I. Röhl, S. Seiffert, S. Shanmugam, V. Sood, J. Soutschek, I. Toudjarska, A. J. Wheat, E. Yaworski, W. Zedalis, V. Kotliansky, M. Manoharan, H.-P. Vornlocher, I. MacLachlan, *Nature* **2006**, *441*, 111.
- [119] A. K. K. Leung, Y. Y. C. Tam, P. R. Cullis, *Adv. Genet.* **2014**, *88*, 71.
- [120] T. Andreussi, C. Galletti, R. Mauri, S. Camarri, M. V. Salvetti, *Comput. Chem. Eng.* **2015**, *76*, 150.
- [121] M. S. Williams, K. J. Longmuir, P. Yager, *Lab Chip* **2008**, *8*, 1121.
- [122] A. D. Stroock, S. K. W. Dertinger, A. Ajdari, I. Mezi, H. A. Stone, G. M. Whitesides, *Science* **2002**, *295*, 647.
- [123] J. B. Knight, A. Vishwanath, J. P. Brody, R. H. Austin, *Phys. Rev. Lett.* **1998**, *80*, 3863.
- [124] A. Jahn, S. M. Stavis, J. S. Hong, W. N. Vreeland, D. L. DeVoe, M. Gaitan, *ACS Nano* **2010**, *4*, 2077.
- [125] A. Jahn, F. Lucas, R. A. Wepf, P. S. Dittrich, *Langmuir* **2013**, *29*, 1717.
- [126] A. Jahn, W. N. Vreeland, D. L. DeVoe, L. E. Locascio, M. Gaitan, *Langmuir* **2007**, *23*, 6289.
- [127] M. Michelon, D. R. B. Oliveira, G. de Figueiredo Furtado, L. Gaziola de la Torre, R. L. Cunha, *Colloids Surf., B* **2017**, *156*, 349.
- [128] M. Guimarães Sá Correia, M. L. Briuglia, F. Niosi, D. A. Lamprou, *Int. J. Pharm.* **2017**, *516*, 91.
- [129] D. Chen, K. T. Love, Y. Chen, A. A. Eltoukhy, C. Kastrup, G. Sahay, A. Jeon, Y. Dong, K. A. Whitehead, D. G. Anderson, *J. Am. Chem. Soc.* **2012**, *134*, 6948.
- [130] E. Kastner, R. Kaur, D. Lowry, B. Moghaddam, A. Wilkinson, Y. Perrie, *Int. J. Pharm.* **2014**, *477*, 361.
- [131] I. V. Zhigaltsev, Y. K. Tam, A. K. K. Leung, P. R. Cullis, *J. Liposome Res.* **2015**, *2104*, 1.
- [132] J. N. Lee, C. Park, G. M. Whitesides, *Anal. Chem.* **2003**, *75*, 6544.
- [133] S. Ramaswamy, N. Tonnu, K. Tachikawa, P. Limphong, J. B. Vega, P. P. Karmali, P. Chivukula, I. M. Verma, *Proc. Natl. Acad. Sci. USA* **2017**, *114*, E1941.
- [134] J. M. Richner, S. Himansu, K. A. Dowd, S. L. Butler, V. Salazar, J. M. Fox, J. G. Julander, W. W. Tang, S. Shresta, T. C. Pierson, G. Ciaramella, M. S. Diamond, *Cell* **2017**, *168*, 1114.
- [135] K. Bahl, J. J. Senn, O. Yuzhakov, A. Bulychev, L. A. Brito, K. J. Hassett, M. E. Laska, M. Smith, Ö. Almarsson, J. Thompson, A. (Mick) Ribeiro, M. Watson, T. Zaks, G. Ciaramella, *Mol. Ther.* **2017**, *25*, 1316.
- [136] B. Li, X. Luo, B. Deng, J. Wang, D. W. McComb, Y. Shi, K. M. L. Gaensler, X. Tan, A. L. Dunn, B. a. Kerlin, Y. Dong, *Nano Lett.* **2015**, *15*, 8099.
- [137] M. A. Oberli, A. M. Reichmuth, J. R. Dorkin, M. J. Mitchell, O. S. Fenton, A. Jaklenc, D. G. Anderson, R. Langer, D. Blankschtein, *Nano Lett.* **2017**, *17*, 1326.
- [138] O. S. Fenton, K. J. Kauffman, R. L. McClellan, E. A. Appel, J. R. Dorkin, M. W. Tibbitt, M. W. Heartlein, F. De Rosa, R. Langer, D. G. Anderson, *Adv. Mater.* **2016**, *28*, 2939.
- [139] N. Pardi, M. J. Hogan, R. S. Pelc, H. Muramatsu, H. Andersen, C. R. DeMaso, K. A. Dowd, L. L. Sutherland, R. M. Searce, R. Parks, W. Wagner, A. Granados, J. Greenhouse, M. Walker, E. Willis, J.-S. Yu, C. E. McGee, G. D. Sempowski, B. L. Mui, Y. K. Tam, Y.-J. Huang, D. Vanlandingham, V. M. Holmes, H. Balachandran, S. Sahu, M. Lifton, S. Higgs, S. E. Hensley, T. D. Madden, M. J. Hope, K. Karikó, S. Santra, B. S. Graham, M. G. Lewis, T. C. Pierson, B. F. Haynes, D. Weissman, *Nature* **2017**, *543*, 248.
- [140] O. S. Fenton, K. J. Kauffman, J. C. Kaczmarek, R. L. McClellan, S. Jhunjhunwala, M. W. Tibbitt, M. D. Zeng, E. A. Appel, J. R. Dorkin, F. F. Mir, J. H. Yang, M. A. Oberli, M. W. Heartlein, F. DeRosa, R. Langer, D. G. Anderson, *Adv. Mater.* **2017**, *29*, 1606944.
- [141] J. B. Miller, S. Zhang, P. Kos, H. Xiong, K. Zhou, S. S. Perelman, H. Zhu, D. J. Siegwart, *Angew. Chem., Int. Ed.* **2017**, *56*, 1059.
- [142] H. Yin, C. Song, J. R. Dorkin, L. J. Zhu, Y. Li, Q. Wu, A. Park, J. Yang, S. Suresh, A. Bizhanova, A. Gupta, M. F. Bolukbasi, S. Walsh, R. L. Bogorad, G. Gao, Z. Weng, Y. Dong, *Nat. Biotechnol.* **2016**, *34*, 328.
- [143] M. Wang, J. A. Zuris, F. Meng, H. Rees, S. Sun, P. Deng, Y. Han, X. Gao, D. Pouli, Q. Wu, I. Georgakoudi, D. R. Liu, Q. Xu, *Proc. Natl. Acad. Sci. USA* **2016**, *113*, 2868.
- [144] X. Zhang, B. Li, X. Luo, W. Zhao, J. Jiang, C. Zhang, M. Gao, X. Chen, Y. Dong, *ACS Appl. Mater. Interfaces* **2017**, *9*, 25481.
- [145] D. C. Montgomery, *Design and Analysis of Experiments*, John Wiley & Sons, Hoboken, NJ **2012**.
- [146] N. Pardi, A. J. Secreto, X. Shan, F. Debonera, J. Glover, Y. Yi, H. Muramatsu, H. Ni, B. L. Mui, Y. K. Tam, F. Shaheen, R. G. Collman, K. Karikó, G. A. Danet-Desnoyers, T. D. Madden, M. J. Hope, D. Weissman, *Nat. Commun.* **2017**, *8*, 14630.
- [147] M. A. Maier, M. Jayaraman, S. Matsuda, J. Liu, S. Barros, W. Querbess, Y. K. Tam, S. M. Ansell, V. Kumar, J. Qin, X. Zhang, Q. Wang, S. Panesar, R. Hutabarat, M. Carioto, J. Hetteringer, P. Kandasamy, D. Butler, K. G. Rajeev, B. Pang, K. Charisse, K. Fitzgerald, B. L. Mui, X. Du, P. Cullis, T. D. Madden, M. J. Hope, M. Manoharan, A. Akinc, *Mol. Ther.* **2013**, *21*, 1570.
- [148] W. C. Tseng, F. R. Haselton, T. D. Giorgio, *J. Biol. Chem.* **1997**, *272*, 25641.
- [149] W. C. Tseng, F. R. Haselton, T. D. Giorgio, *Biochim. Biophys. Acta, Gene Struct. Expression* **1999**, *1445*, 53.
- [150] I. MacLachlan, P. Cullis, R. W. Graham, *Curr. Opin. Mol. Ther.* **1999**, *1*, 252.

- [151] J. van der Oost, M. M. Jore, E. R. Westra, M. Lundgren, S. J. J. Brouns, *Trends Biochem. Sci.* **2009**, *34*, 401.
- [152] M. Jinek, A. East, A. Cheng, S. Lin, E. Ma, J. Doudna, *Elife* **2013**, *2*, e00471.
- [153] F. A. Ran, P. D. Hsu, J. Wright, V. Agarwala, D. A. Scott, F. Zhang, *Nat. Protoc.* **2013**, *8*, 2281.
- [154] H. Yin, W. Xue, S. Chen, R. L. Bogorad, E. Benedetti, M. Grompe, V. Kotliansky, P. A. Sharp, T. Jacks, D. G. Anderson, *Nat. Biotechnol.* **2014**, *32*, 551.
- [155] D. Haussecker, *FEBS J.* **2016**, *283*, 3249.
- [156] E. Oude Blenke, M. J. W. Evers, E. Mastrobattista, J. van der Oost, *J. Controlled Release* **2016**, *244*, 139.
- [157] Silence Therapeutics, CRISPR/Cas9 gene editing data, <http://silence-therapeutics.com/media/1162/st-crispr-15nov16.pdf> (accessed: September 2017).
- [158] Intellia Therapeutics, Strategy, <http://www.intelliatx.com/strategy/> (accessed: September 2017).
- [159] *Nat. Biotechnol.* **2014**, *32*, 961.